FACILITY FORM 602

(ACCESSION NUMBER) 57	(THRU) NONE
(PAGES) CR-112380	(CODE)
(NASA CR OR TMX OR AD NUMBER)	(CATEGORY)

1450 S. ROLLING ROAD, BALTIMORE MD, 21227 • PHONE A.C. 301, 247-0700

Band Structure and Bonding In Titanium Carbide

Second Technical Report to NASA

by
Robert G. Lye

National Aeronautics and Space Administration
Contract NASw-1290

RIAS Technical Report 66-8

November 1966

Research Institute for Advanced Studies
(RIAS)
Martin Marietta Corporation
1450 South Rolling Road
Baltimore, Maryland 21227

Abstract.

The two-center LCAO method, which has been used frequently in the past to study the motion of electrons in solids, is used here to investigate the nature of bonding between atoms in TiC. It is found that prominent contributions to the bonding in this material arise from metal-metal interactions similar to those in the transition metals. In TiC, however, these interactions are strengthened by the effect of carbon atom core potentials in the regions of overlap between metal orbitals. Moreover, the number of electrons participating in such interactions is increased by electrons transferred from carbon to metal orbitals. Additional bonding, with substantial covalent character, is contributed by the carbon atoms as a result of metal-carbon and carbon-carbon interactions. Ionic interactions also are present because of the electron transfer between atoms, but they appear to contribute little to the cohesive energy of TiC.

These results provide support for proposals advanced by Kiessling and by Robins to explain the bonding in refractory hard metals. They are not in accord with the explanation offered by Rundle.

It is suggested that the close relationship between band structure and bonding illustrated here for TiC can be used to advantage also in studies of the bonding in transition metals and in other materials that exhibit complex bonding characteristics.

Band Structure and Bonding in Titanium Carbide.

I. Introduction.

The properties of solids may be described either in terms of energy bands or in terms of chemical bonds. Although accurate calculations of electronic energy bands in a solid provide sufficient information to explain many physical properties, the results of such calculations are somewhat unsatisfactory for visualizing the bonding between atoms of the solid. The chemical bond approach, on the other hand, although less satisfactory for quantitative calculations of physical properties, does provide a useful representation of the bonding.

Several years ago, Hall (1) and Slater (2) suggested ways in which crystal wave functions determined from energy band calculations might be combined to generate equivalent bond orbitals closely related to those used in the chemical bond description, but little use appears to have been made of this correspondence between the two approaches. One reason for this is the fact that the equivalent orbitals often are not describable in simple form. Nevertheless, even a qualitative analysis of the bonding may be valuable for understanding certain physical properties, particularly of those compounds in which complex mixtures of various types of bonding occur. The purpose of this paper is to present for one such compound, TiC, a preliminary description of the bonding which has been obtained directly from calculations of its energy band structure. The present description is incomplete because only those components of the equivalent orbitals have been included that provide the more

prominent contributions to bonding. Subsequent work, however, will be directed toward calculation of complete equivalent orbitals in the manner suggested by Slater and Hall.

Titanium carbide was chosen for this study because the nature of its bonding has been the subject of speculation for many years. It is one of the more familiar members of a group of substances, commonly referred to as refractory hard metals, that are formed by reacting a transition metal from Groups IV to VI with one of the small nonmetallic elements such as boron, carbon, nitrogen, and oxygen. The unusual properties of these compounds have been discussed in detail by Schwarzkopf and Kieffer (3) and by Kieffer and Benesovsky (4): Together with the high melting point and great hardness characteristic of such covalent solids as diamond, they exhibit electrical conductivities comparable with those of the parent transition metals (5). Such a combination of covalent and metallic properties has led to rather divergent opinions regarding the nature of these compounds.

Possibly the earliest consideration given to the problem occurred in 1931 during Ubbelohde's study (6) of the palladium-hydrogen system, from which he inferred that hydrogen donated electrons to fill holes in the d band of palladium. Ubbelohde then suggested that nonmetal atoms in other interstitial compounds of the transition metals might behave in the same way. In 1943, Umanskii (7) discussed the hardness of interstitial phases and the electromigration of carbon and nitrogen in iron. He concluded that Ubbelohde's views applied in these circumstances also. Rundle, on the other hand, proposed in 1948 (8) that for refractory hard metals the electron transfer was in the other

direction, that is, from the metal to the nonmetal atom. He argued that, because the metal-metal atom spacings generally are greater in the refractory hard metals than in the parent transition metals, the metal-metal bonds must be weaker in the hard metals than they are in the parent metals. Thus, he suggested that electrons must have been lost from the metal-metal bonds, and accordingly attributed the increased melting points, hardness and brittleness of the hard metals to the formation of strong directional bonds between metal and nonmetal atoms. Subsequent experimental work by Kiessling (9) indicated, however, that electrons are transferred from the nonmetal to the metal atom. Kiessling (10), in 1957, proposed, therefore, that the bonding in hard metals is essentially metallic in nature, but suggested that covalent and ionic bonding also may be present in certain of these compounds. Robins (11) presented a similar model for the bonding in 1958, but emphasized the effects of electron concentration and coordination of the metal atoms.

In 1958, Bilz (12) attempted to distinguish between the alternatives of strong metal-nonmetal bonding (Rundle) and strong metal-metal bonding (Kiessling and Robins) by considering the properties expected in each case for a (hypothetical) titanium hard metal, TiX, related to TiC, TiN, and TiO, and having the same rocksalt structure. For each type of bonding, he estimated the distribution in energy of electronic states in a molecular unit, Ti_6X, having the same atomic configuration that it would have in a crystal of TiX. The resulting density-of-states curves were compared with an equivalent curve obtained from a calculation of the electronic energy band structure for the hypothetical TiX crystal. This calculation was performed following

the simplified LCAO (linear combination of atomic orbitals) method of Slater and Koster (13), which will be discussed later. For the interaction integrals of TiX required in the calculation, Bilz used values estimated from previous calculations for nickel and copper; for the one-electron energies of the X atom he used the average of values for carbon, nitrogen, and oxygen. He concluded that the density-of-states curve obtained from this calculation represented an intermediate condition in which the bonding included both metal-metal and metal-nonmetal interactions. His band structure requires a substantial transfer of electrons from states of the metal atom to states of the nonmetal atom, and thus supports the model proposed by Rundle.

Dempsey (5), in 1963, presented arguments that support Kiessling's description of the refractory hard metals. Dempsey discussed similarities between the properties of transition metals and refractory hard metals that have approximately equal numbers of d electrons. He concluded that the close correlations observed could be accounted for if (i) the bonding in refractory hard metals is similar to that in transition metals, and (ii) electrons are transferred to the transition metal d band from the nonmetal atoms. Dempsey suggested also that covalent bonding involving the nonmetal atoms does not play an important role; thus, his analysis leads to conclusions almost opposite to those of Rundle.

More recently (1964), Costa and Conte (14) computed band structures for TiC and TiN using the Fletcher (15) approach to the LCAO method. Their calculations indicated a considerable strengthening of the interactions between metal d orbitals by the potential of carbon atoms located in their vicinity - an important effect which had not been considered previously. Accordingly Costa

and Conte suggested that metal-metal interactions were more important than Bilz had supposed, but they acknowledged that few experimental data then available contradicted Bilz's band structure.

In 1965, Ern and Switendick (16) computed separate band structures for TiC, TiN, and TiO using the APW (augmented plane wave) method. Their results supported in most respects the earlier calculations by Bilz.

Unfortunately, these models for the refractory hard metals could not be evaluated adequately in the past because of the lack of appropriate experimental data. Recently, however, some of the required information has been made available for TiC from Logothetis' (17) determination of its optical properties over a wide range of photon energies. These data have been used by Lye (17) to guide new LCAO calculations of an electronic energy band structure for this material, and the results have been employed to develop a description of the bonding in TiC. Although this new band structure is markedly different from those obtained from previous calculations, the nature of the bonding it implies includes aspects of most of the earlier descriptions, differing from them primarily in emphasis.

In the present paper, the LCAO method and its relation to familiar concepts of bonding will be described in Section II. The band structure for TiC computed using this method will then be discussed in Section III, and a qualitative description of the bonding inferred from the calculations will be given in Section IV. This model for the bonding in TiC will be discussed with reference to its physical properties in Section V.

II. Band Structure Calculations by the LCAO Method.

A useful approximation to the electron energy band structure of TiC may be obtained using the simplified two-center LCAO (linear combination of atomic orbitals) method suggested by Slater and Koster. The LCAO method has been described extensively elsewhere (13, 18-22); only qualitative aspects will be discussed here. In this discussion, however, mathematical arguments will be presented, where possible, in pictorial form to illustrate this technique for computing electronic energy bands and to demonstrate visually the bonding which results from interactions between atomic orbitals.

In the LCAO approximation, crystal wave functions are constructed from atomic wave functions (orbitals) which are centered on the sites, R_j, of the crystal lattice. The atomic orbitals contribute to the crystal wave function of wave vector k according to the complex weighting factor $\exp(ik\cdot R_j)$, which establishes for each value of k and R_j the phase of the orbital at R_j with respect to the one on the atom chosen as the origin. Spherically symmetric atomic s functions, $\varphi_s(r)$, for example, form crystal wave functions, $\Phi_s(k,r)$, which are represented (as Bloch functions) in the form:

$$\Phi_s(k,r) = \sum_j \exp(ik\cdot R_j)\varphi_s(r-R_j).$$

That is, around each atom of the solid, at the lattice sites labeled R_j, the crystal wave function looks much like the original atomic s function. In particular, at the center of the Brillouin zone (k=0), the crystal wave function

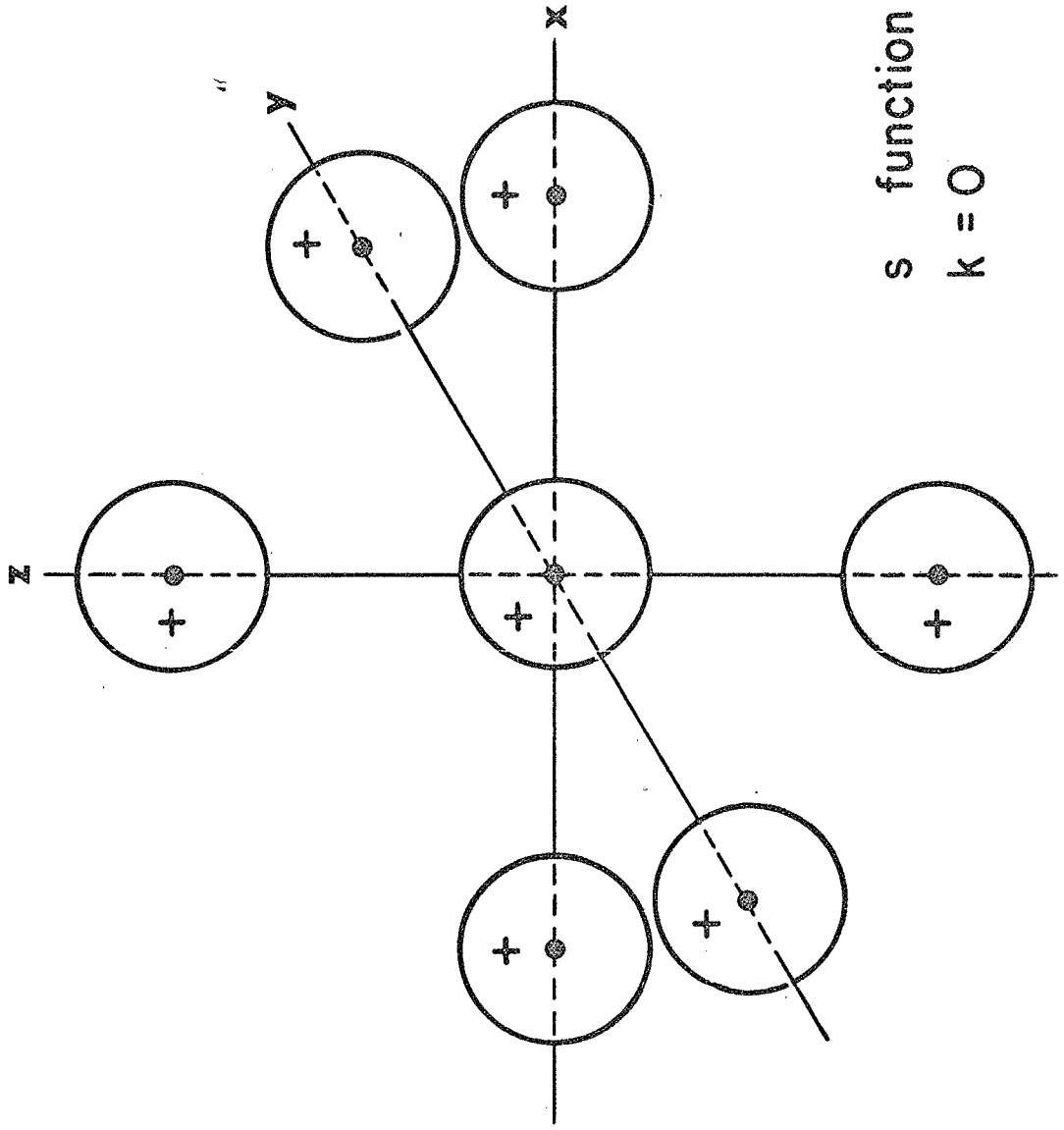

Fig. 1. - Crystal wave function for the center of the Brillouin zone, Γ (k=0), constructed from atomic orbitals of spherical symmetry (atomic s functions) centered on the atoms of a simple cubic crystal. Separation of the atoms is exaggerated for clarity.

is approximately an array of atomic s functions with the same phase on each atomic site, as shown in Fig. 1 for a simple cubic crystal. (The orbitals are drawn reduced in size for clarity; some overlap between them is necessary to permit interactions to occur.)

Atomic orbitals on one atom overlap onto adjoining atoms and interact with the orbitals on those atoms through the total potential, $V(r) = \sum_{j\neq 0} V_a(r-R_j)$, which is the sum of atomic potentials, $V_a(r-R_j)$, from all the neighboring atoms. The strength of the interaction, $J(R_B)$, between the wave functions $\varphi_A(r)$ on atom A and $\varphi_B(r-R_B)$ on atom B, displaced by the vector R_B from A, is determined by integrating the products of the wave functions and the potential over the volume of the crystal, τ, in which the wave functions overlap:

$$J(R_B)=\int \varphi_B^*(r-R_B) \sum_{j\neq 0} V_a(r-R_j)\varphi_A(r)d\tau .$$

In the two-center approximation, the principal contribution to the potential is assumed to arise from just the atom on which the interacting wave function resides. This simplification permits the interactions to be described in terms of the two-center integrals,

$$\int \varphi_B^*(r-R_B)V_B(r-R_B)\varphi_A(r)d\tau$$

familiar from the study of diatomic molecules. Moreover, this approach leads directly to a pictorial representation of the bonding in solids which is closely analogous to the common description of bonding in molecules.

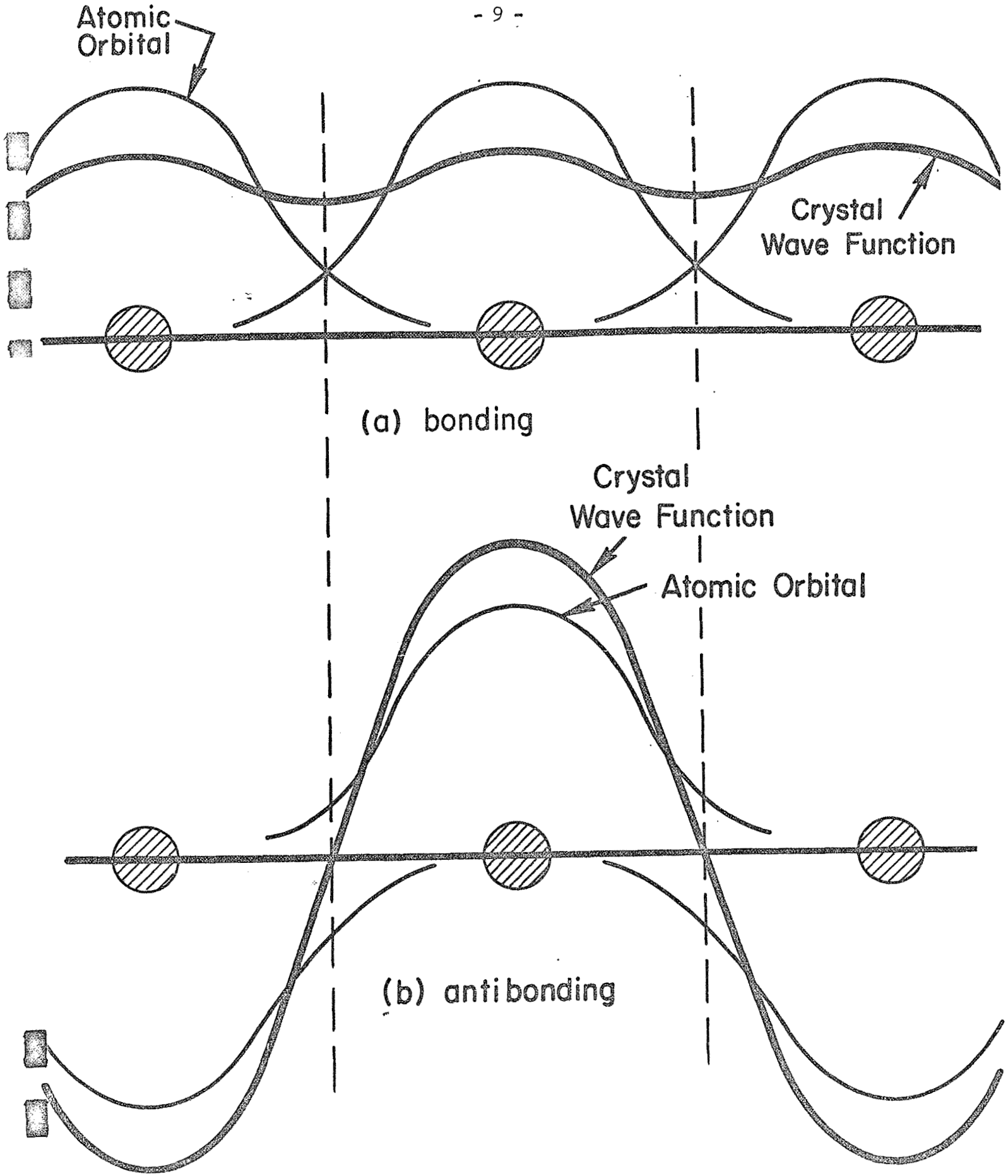

Fig. 2. - Interactions between atomic orbitals: (a) bonding, (b) antibonding.

For the purposes of this discussion, it is necessary to employ a specific meaning for the term "bonding". The term has been used in a variety of ways in the literature, sometimes with essentially the same meaning as cohesive energy. However, a distinction will be made between the two terms in what is to follow: Cohesive energy will be used in the usual way to designate the difference (at $0^{\circ}K$) between the energy of one mole of isolated atoms and the energy of those atoms when assembled in the periodic configuration they assume in the solid state. The terms "bonding" and "antibonding", on the other hand, will be used to describe interactions between atoms in the solid array. Bonding due to electrostatic interactions between atoms is the familiar ionic bonding, and can be correlated with the ionic contribution to the cohesive energy. The electronic contribution to bonding results from interactions between wave functions associated with different atoms and can be either bonding or antibonding. Overlap of functions with the same sign decreases their energy by increasing the amplitude near the boundary of the polyhedron surrounding the atom and decreasing the amplitude inside (since $\int \varphi^* \varphi d\tau$ is a constant within the polyhedron). The wave function is made smoother by the overlap, as shown in Fig. 2(a); thus, the kinetic energy, $\frac{\hbar^2}{2m} \int |\text{grad}\varphi|^2 d\tau$, is decreased (18). The amount of the decrease is determined by the magnitude of the two-center integral representing this interaction. Bonding that results from such interactions is determined in the same way as is the change in electronic energy: Since the electronic energy is lowered by overlap of orbitals with <u>like sign,</u> the energy is decreased by bringing the atoms together; thus, the atoms are attracted to each other by <u>bonding</u> interactions. Conversely, the electronic energy is increased when orbitals of

opposite sign overlap, as shown in Fig. 2(b); under such circumstances, the atoms repel each other by antibonding interactions. This component of bonding between atoms can be calculated, therefore, from the same two-center integrals that determine the change in electronic energy. The cohesive energy that results can be considered either as the sum of interactions between atoms or as the net change in energy of the electrons.

Atomic s states. The two-center approximation thus provides a means for computing the electronic energy bands in a solid and, at the same time, indicates the nature of the bonding between atoms. For example, the interaction between the central atom and each of its nearest neighbors in Fig. 1 can be represented by the quantity

$$ss\sigma_a = \int \varphi_s^*(r-a) V(r-a) \varphi_s(r) d\tau$$

in which the symbol $ss\sigma_a$ indicates a sigma interaction between two s functions on atoms a distance a apart. (Similar nomenclature will be used later for the two-center integrals representing interactions between other atomic functions.) In the two-center approximation, the total change in energy of the electron relative to its energy in an isolated atom is a simple sum of the contributions from interactions between one orbital and all nearby orbitals. Since the orbital on the central atom in Fig. 1 has the same phase, indicated by the plus sign, as those on the six neighboring atoms, it forms bonding $ss\sigma$ interactions with each of these orbitals. As a result, the energy

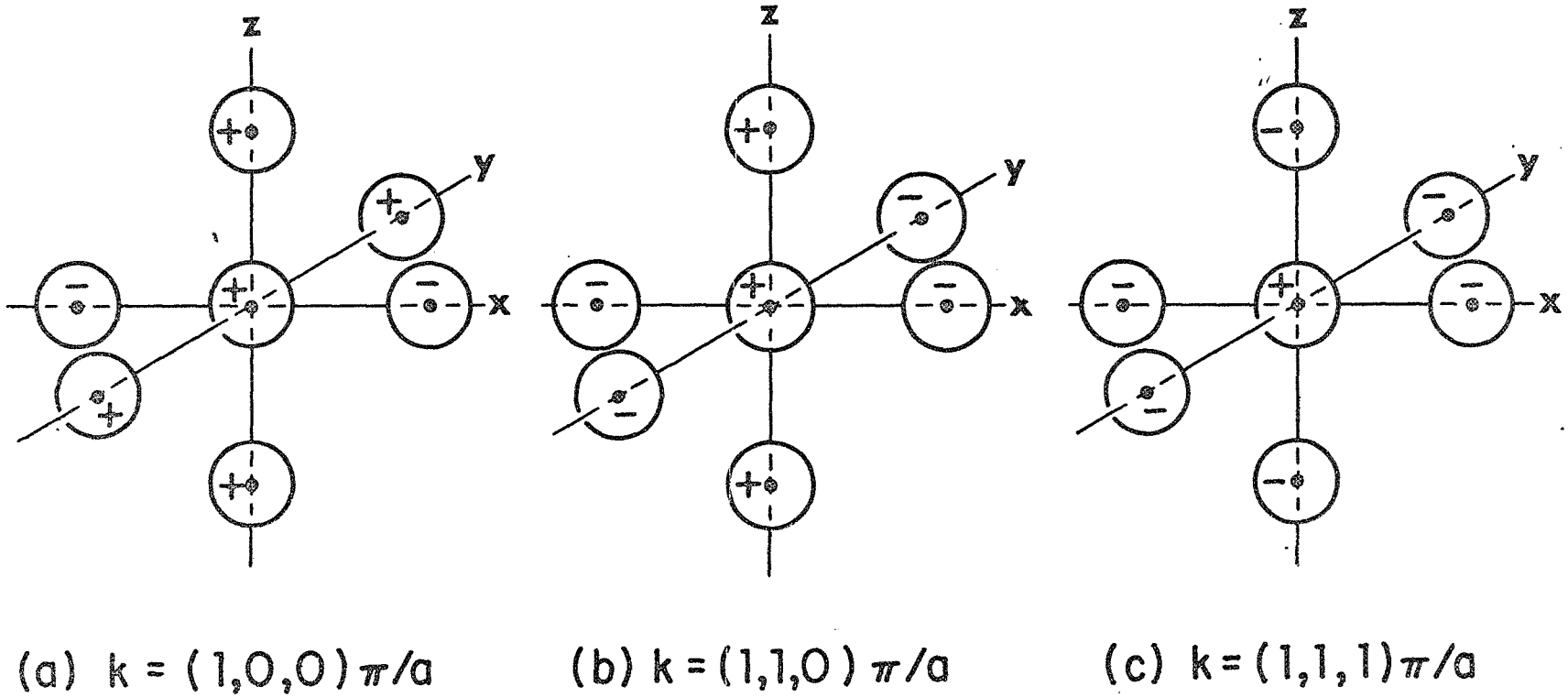

Fig. 3. - Crystal wave functions constructed from atomic s orbitals on the atoms of a simple cubic crystal with lattice constant a. Phases of atomic orbitals on nearest neighbor atoms are shown at three points of high symmetry on the surface of the Brillouin zone: (a) Crystal wave function for $k=(1,0,0)\pi/a$. Phase changes occur only along the x direction in the crystal. (b) Crystal wave function for $k=(1,1,0)\pi/a$. Phase changes occur along the x and y directions, but not along the z direction. (c) Crystal wave function for $k=(1,1,1)\pi/a$. Phase changes occur along x, y, and z directions.

of the crystal wave function, represented in the figure for k=0, is depressed by $6|ss\sigma_a|$ from the energy of the s state in the free atom.

When the momentum of the crystal wave function differs from zero, the orbitals on atoms at lattice sites R_j have to be multiplied by appropriate phase factors, $\exp(ik\cdot R_j)$. Crystal wave functions that result are illustrated schematically in Fig. 3 for wave vectors at the Brillouin zone boundaries, $k=(1,0,0)\pi/a$, $k=(1,1,0)\pi/a$, and $k=(1,1,1)\pi/a$, of a simple cubic crystal with lattice spacing a. When $k=(1,0,0)\pi/a$, Fig. 3(a), the phase factor changes by $e^{\pm i\pi}=-1$ for every lattice translation $\pm$ a along the x direction in the crystal, but it is the same for all atoms in each y-z plane. The four nearest neighbors in the y-z plane have the same sign as the central atoms and are again in bonding configuration. Orbitals on the two atoms at $(\pm a,0,0)$, however, have the opposite sign; thus, they are in antibonding configurations relative to the one on the central atom. The four bonding and two antibonding interactions provide a net contribution of two bonding $ss\sigma$ interactions. The state $k=(1,0,0)\pi/a$ is, therefore, only one-third as strongly bonded as the state k=0.

When $k=(1,1,0)\pi/a$, the s function on each atom is in bonding configuration with two of its nearest neighbors at $(0,0,\pm a)$ and in antibonding configuration with four at $(\pm a,0,0)$ and $(0,\pm a,0)$ to produce a net contribution of two antibonding $ss\sigma$ interactions. When $k=(1,1,1)\pi/a$, the s function on each atom participates in six antibonding $ss\sigma$ interactions with its nearest neighbors. Equivalent results, of necessity, are obtained from direct calculations of the

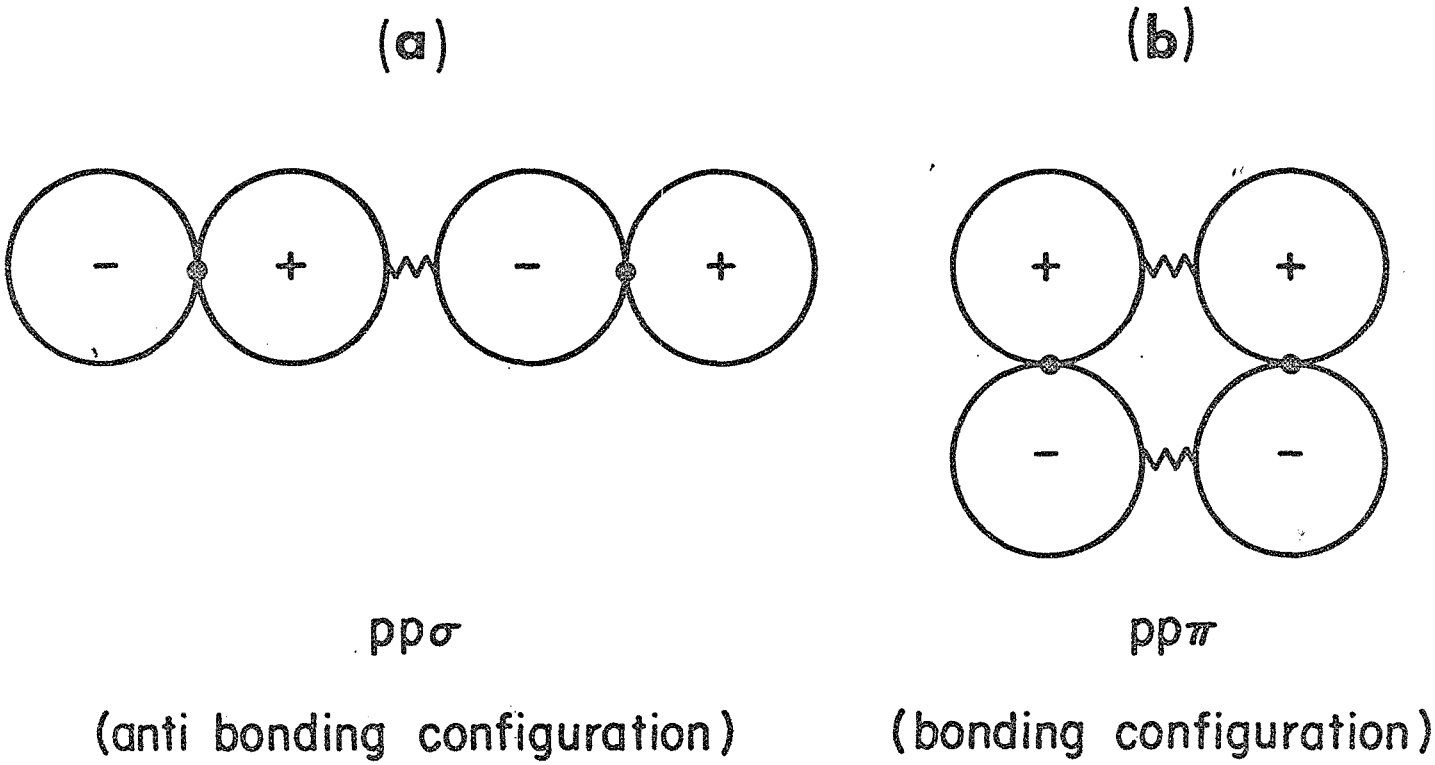

Fig. 4. - Atomic p functions: (a) in σ orientation, principal axes along the line joining atom centers; and (b) in π orientation, principal axes perpendicular to the line joining atom centers. For arbitrary orientations of p functions, interactions between them are computed by resolving each into σ and π components.

Table I

k (units of π/a)	Energy	Net ssσ bonding with nearest neighbors
0,0,0	$s_o+6ss\sigma_a$	6 bonding
1,0,0	$s_o+2ss\sigma_a$	2 bonding
1,1,0	$s_o-2ss\sigma_a$	2 antibonding
1,1,1	$s_o-6ss\sigma_a$	6 antibonding

Table I: Electronic energy and atomic bonding of s functions in a simple cubic lattice calculated by the nearest-neighbor, two-center, LCAO approximation. s_o is approximately the energy of the s state in an isolated atom.

energy using the nearest-neighbor two-center LCAO approximation, which provides the mathematical basis for this description of bonding. Energies calculated in this way for crystal wave functions formed from an atomic s state are listed in Table I for points in the Brillouin zone at which the bonding has been discussed. The degree of bonding between s functions on nearest neighbor atoms is listed for comparison.

At an intermediate point in the Brillouin zone, $k=(k_x,k_y,k_z)$, the wave functions are multiplied by complex phase factors, $\exp(ik\cdot R_j)$. The result is not readily presented pictorially, but the energy and bonding can be calculated directly: Wave functions on the two atoms at $(\pm a,0,0)$ have phase factors $\exp(\pm ik_x a)$ and the sum of interaction between these two wave functions and the one on the central atom is $ss\sigma_a[\exp(ik_x a)+\exp(-ik_x a)]=2ss\sigma_a \cos k_x a$. Similarly, wave functions on the two atoms at $(0,\pm a,0)$ have phase factors $\exp(\pm ik_y a)$ and the sum of their interactions with the wave function on the central atom is $2ss\sigma_a \cos k_y a$. In the same way, the two atoms at $(0,0,\pm a)$ contribute $2ss\sigma_a \cos k_z a$. The total interaction with the six nearest neighbors is, therefore, $2ss\sigma_a(\cos k_x a+\cos k_y a+\cos k_z a)$. The energy and bonding thus vary continuously through the Brillouin zone from the lowest energy (strongest bonding) at $k=0$ to the highest energy (strongest antibonding) at $k=(1,1,1)\pi/a$.

Atomic p states. If the outer atomic states are p states, the energy of crystal wave functions formed from them and the bonding interactions between them vary with momentum in a different way. The atomic p state is triply degenerate, that is, the three states with wave functions $xf(r)$, $yf(r)$, and $zf(r)$, have the

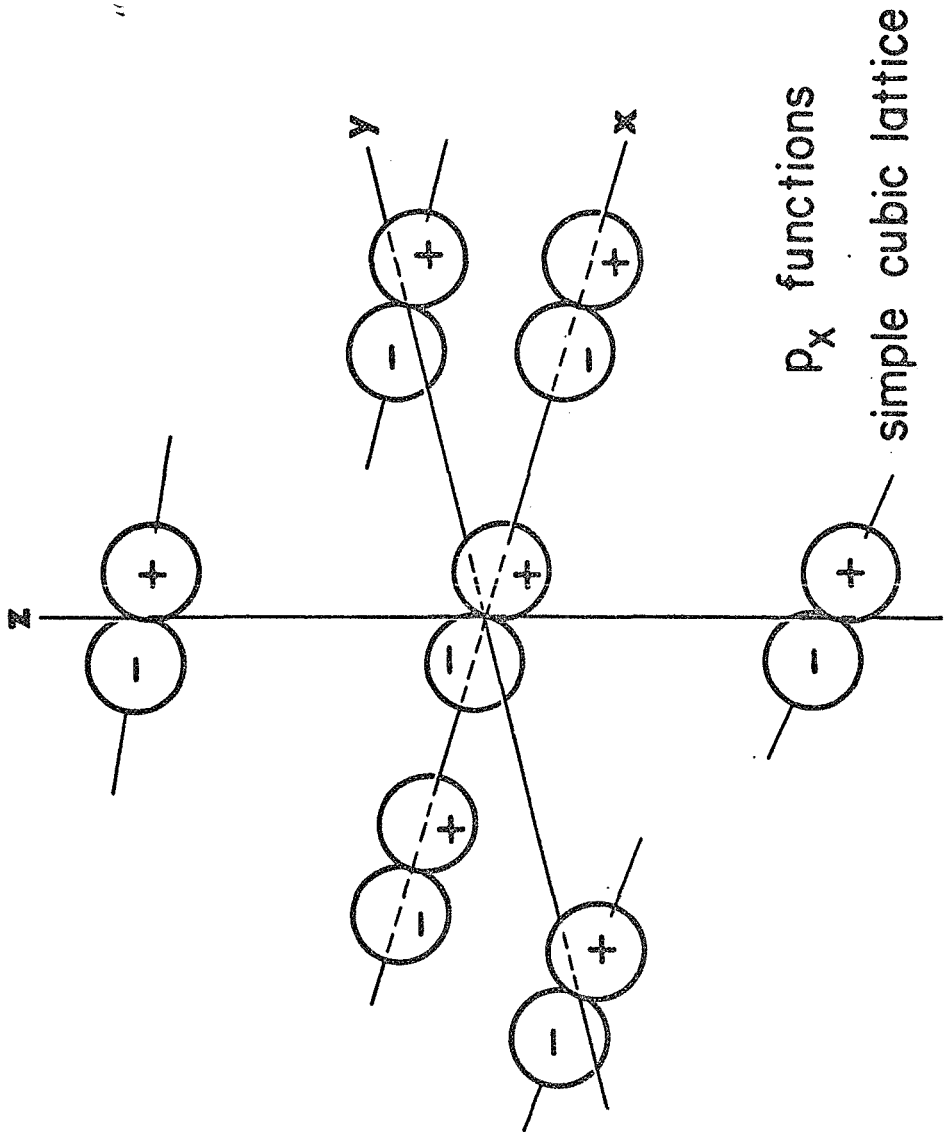

Fig. 5. - Crystal wave function for k=0 constructed from atomic p_x orbitals centered on the atoms of a simple cubic crystal with lattice constant a. All orbitals have the same phase. Orbitals on nearest neighbor atoms in the y-z plane form $pp\pi$ bonding interactions with the central orbitals. Orbitals at $\pm a$ in the x direction form $pp\sigma$ antibonding interactions.

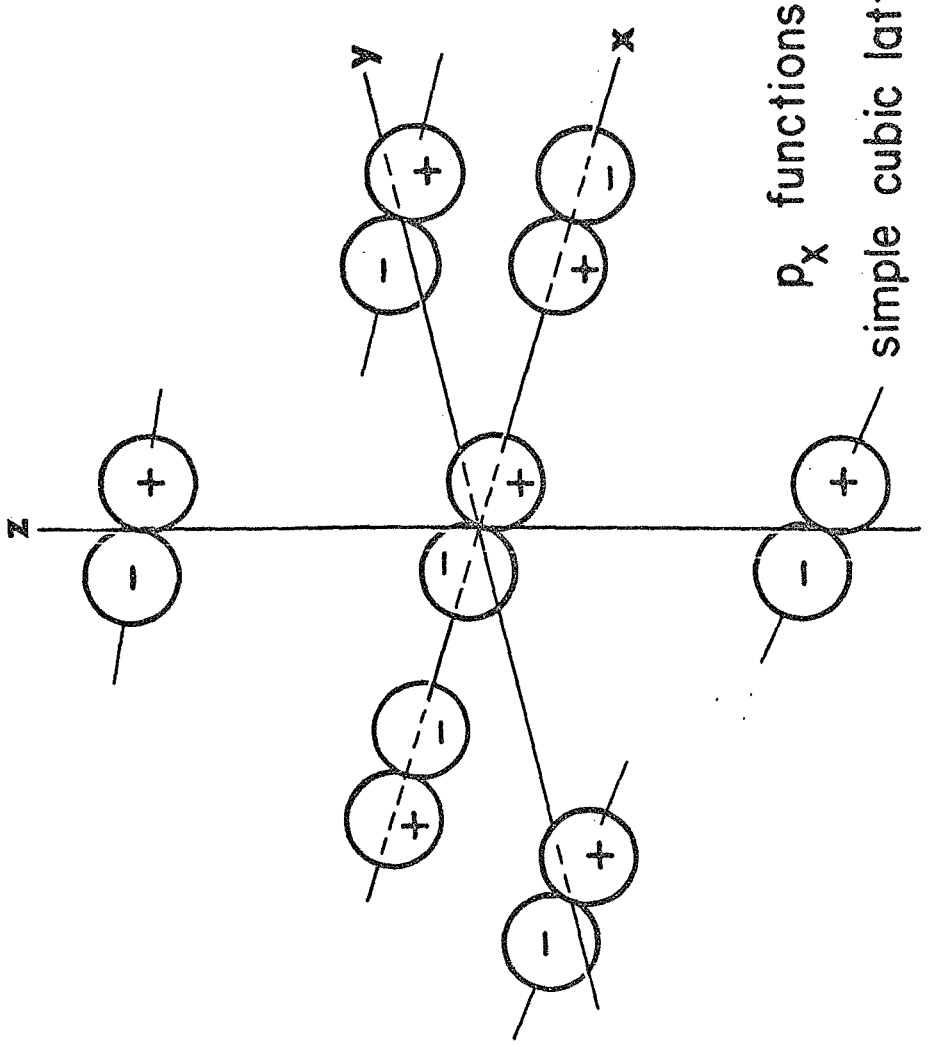

Fig. 6. - Crystal wave function constructed from atomic p_x orbitals centered on the atoms of a simple cubic crystal with lattice constant a. Phases of atomic orbitals on nearest neighbor atoms are shown for $k=(1,0,0)\pi/a$. Changes of phase occur along the x-direction in the crystal, but all orbitals in each y-z plane have the same phase. As for k=0, Fig. 5, orbitals on nearest neighbor atoms in the y-z plane form $pp\pi$ bonding interactions, but orbitals at $\pm a$ in the x direction now form bonding $pp\sigma$ interactions.

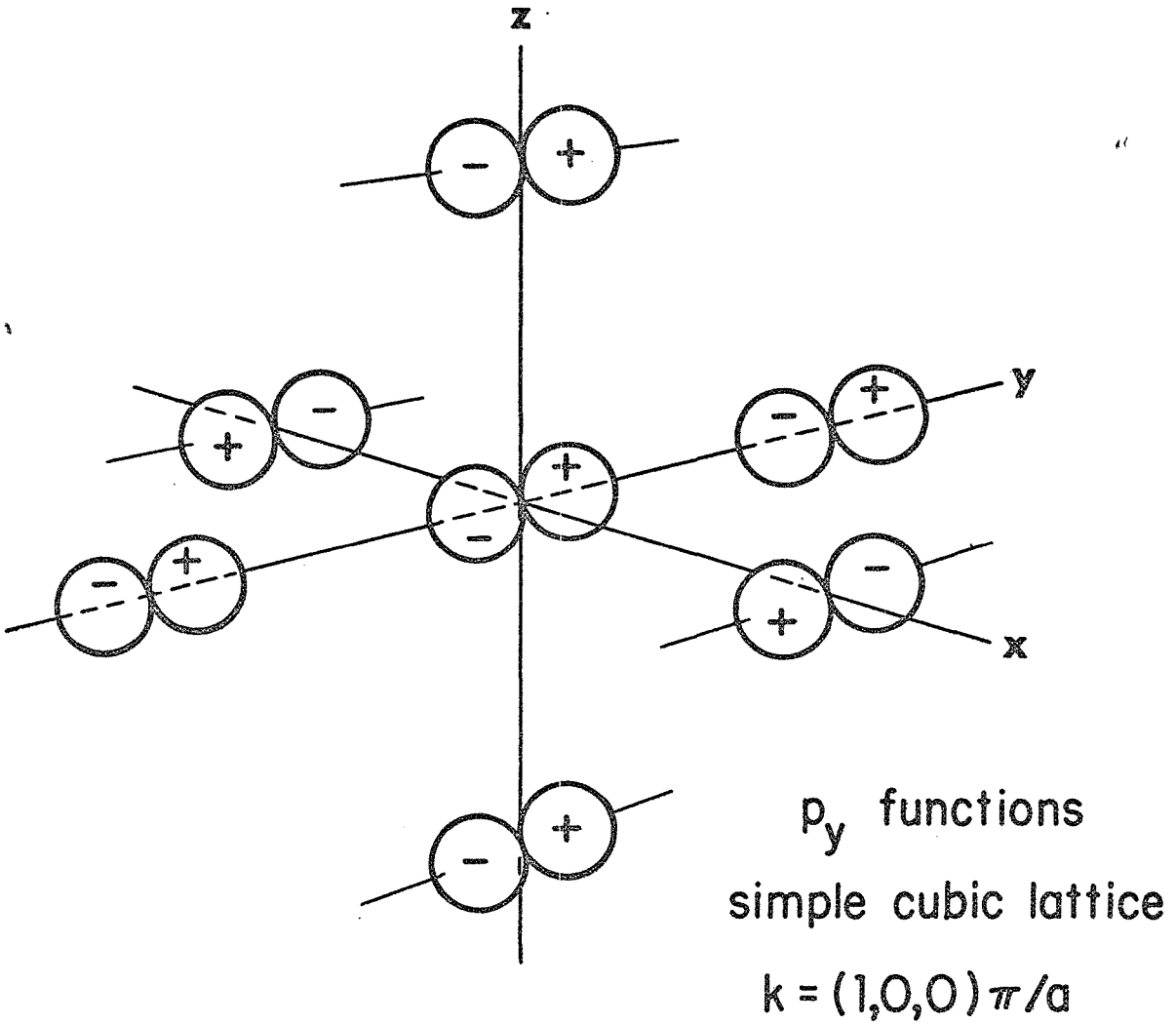

Fig. 7. - Crystal wave functions constructed from atomic p_y orbitals centered on the atoms of a simple cubic crystal with lattice constant a. Phases of atomic orbitals are shown for $k=(1,0,0)\pi/a$. Changes of phase occur along the x direction in the crystal, but all orbitals in each y-z plane have the same phase. The four p_y orbitals in the x-z plane form antibonding $pp\pi$ interactions, and the two at $\pm a$ in the y direction form antibonding $pp\sigma$ interactions. This strongly antibonding configuration of atomic orbitals represents a crystal wave function of high energy.

same energy in the free atom. Two types of p-p interactions are possible, the $pp\sigma$ and the $pp\pi$ interactions illustrated in Fig. 4. The p functions shown in σ orientation are in the $pp\sigma$ antibonding configuration whereas the π oriented functions are bonding. Note, however, that the σ oriented functions would become bonding and the π oriented functions antibonding by reversing the signs of one function in each pair.

Fig. 5 shows the configuration of p_x functions in a simple cubic lattice for k=0. The central atom interacts with its nearest neighbors along the x axis to form two antibonding $pp\sigma$ bonds, and forms four bonding $pp\pi$ bonds with nearest neighbors in its y-z plane. The p_y and p_z functions behave in the same way at k=0; the p functions remain triply degenerate for this value of momentum. Fig. 6 shows the configuration of p_x functions at $k=(1,0,0)\pi/a$. In this case, the central atom again makes four bonding $pp\pi$ interactions with neighboring atoms in its y-z plane, but now is in bonding $pp\sigma$ configuration with the two neighboring atoms in the x direction. The p_y functions behave quite differently, as shown in Fig. 7. The p_y function on the central atom makes two antibonding $pp\pi$ interactions in the $\pm x$ direction, two bonding $pp\pi$ interactions in the $\pm z$ direction, and two antibonding $pp\sigma$ interactions in the $\pm y$ direction. Thus, the p_y functions are antibonding at $k=(1,0,0)\pi/a$, whereas the p_x functions are in bonding configuration at this point in the Brillouin zone. The p_z functions are degenerate with the p_y functions along the (1,0,0) direction in the Brillouin zone.

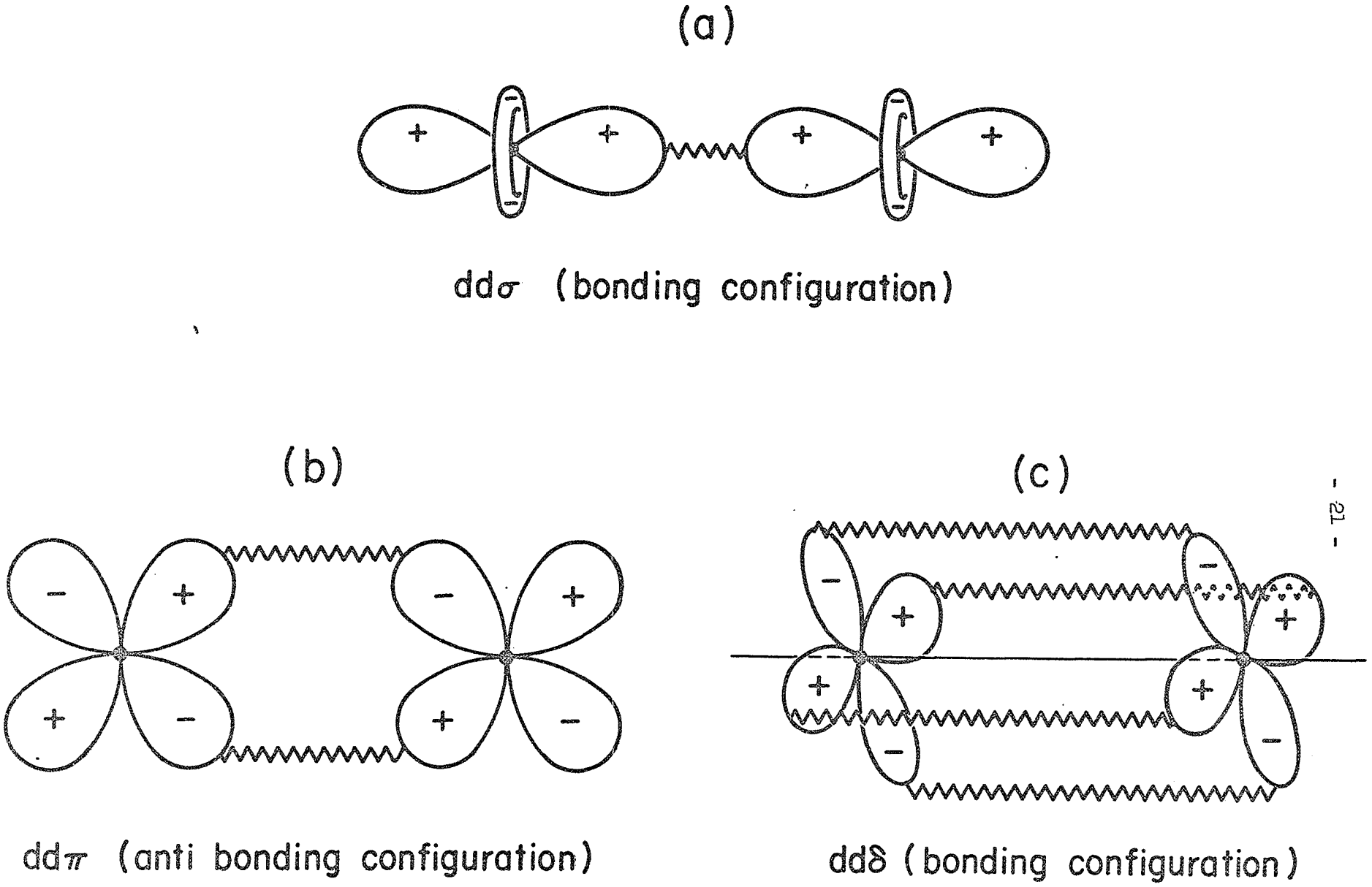

Fig. 8. - Atomic d functions: (a) in σ orientation, principal axes along the line joining atom centers; (b) in π orientation, principal axes in a plane through the line joining atom centers; and (c) in δ orientation, principal axes in planes perpendicular to the line joining atom centers. For arbitrary orientations of d functions, interactions between them are computed by resolving each into σ, π, and δ components.

Atomic d states. Three types of interactions are possible for d functions, $dd\sigma$, $dd\pi$, and $dd\delta$, as illustrated in Fig. 8. The interaction of two d functions frequently involves all three types of bonding. Magnitudes of the separate contributions can be calculated by resolving the functions into σ, π, and δ components. The results are available in Table I of the paper by Slater and Koster (13).

Hybrid interactions. When outer electronic states of different symmetry have comparable energies in the isolated atom, it is no longer possible to consider separately the crystal wave functions derived from these states because interactions between them are possible for certain values of their momenta. As a result of such interactions, the crystal wave functions become hybridized and contain contributions from each of the interacting states. Each of the n different crystal functions, $\Psi_n(k,r)$, formed from the n atomic states, $\varphi_m(r)$, is then written as a sum of Bloch functions, $\Phi_m(k,r)$:

$$\Psi_n(k,r)=\Sigma_m a_{mn}(k)\Phi_m(k,r),$$

in which

$$\Phi_m(k,r)=\sum_j \exp(ik\cdot R_j)\varphi_m(r-R_j),$$

as for the s functions discussed before. In this case, however, the Bloch functions, $\Phi_m(k,r)$, have to be constructed, not from simple atomic functions, but from appropriate combinations of the atomic function on the central atom and other functions on the surrounding atoms. These (orthogonalized) combinations retain the symmetry of the wave function on the central atom;

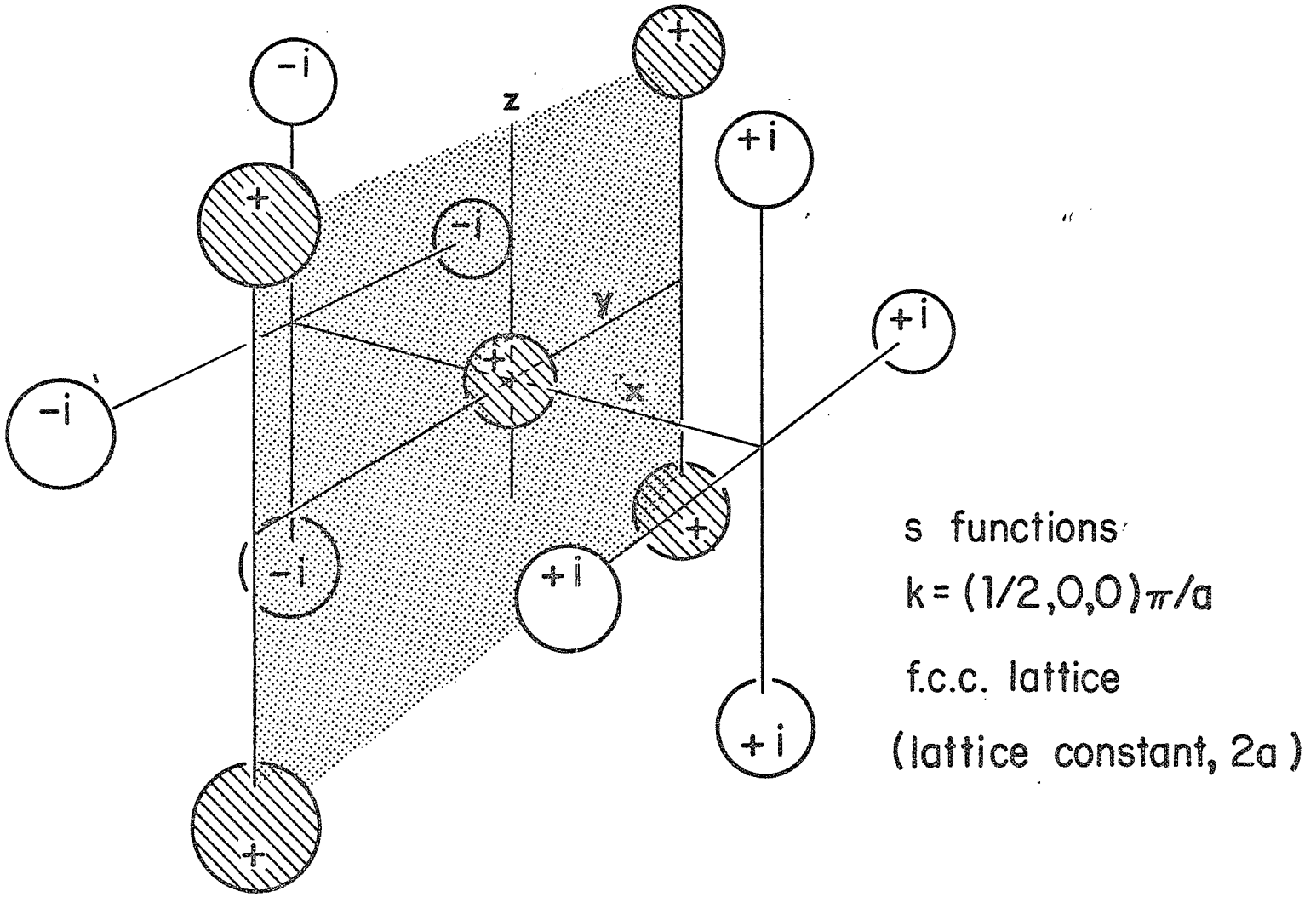

Fig. 9. - Crystal wave function constructed from atomic s orbitals centered on the atoms of a face-centered-cubic crystal with lattice constant 2a. Phases of atomic orbitals are shown for $k=(1/2,0,0)\pi/a$. All orbitals in each y-z plane have the same phase, but the phase changes by $\exp(\pm i\pi/2)=\pm i$ for each translation $\pm a$ along the x direction in the crystal. The four orbitals on neighboring atoms in the y-z plane form bonding ssσ interactions with the central atoms. Interactions made by the central orbital with orbitals in the plane at x=+a are cancelled by interactions with orbitals in the plane x=-a for $k=(1/2,0,0)\pi/a$.

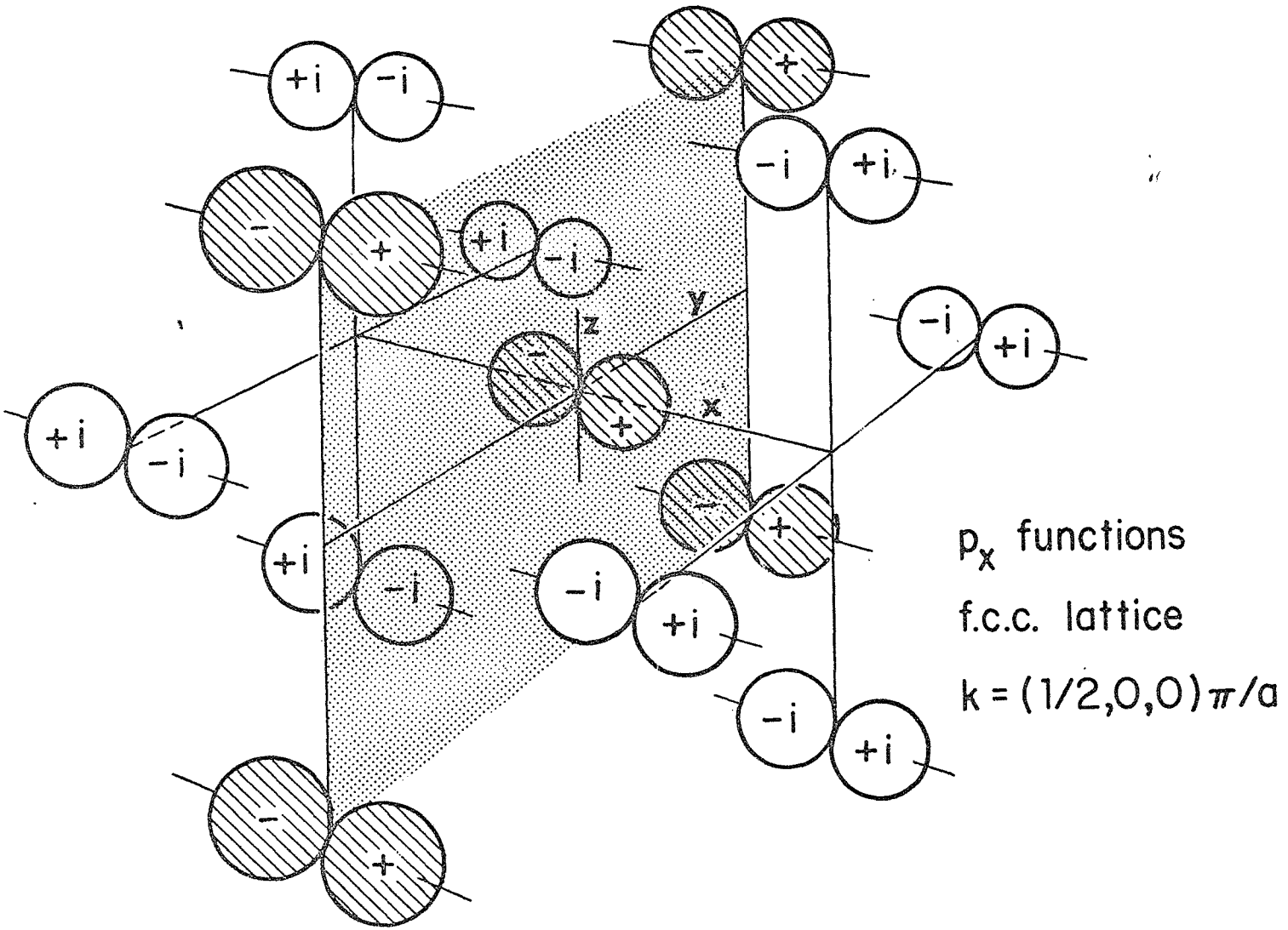

Fig. 10. - Crystal wave functions constructed from atomic p_x orbitals centered on the atoms of a face-centered-cubic crystal with lattice onstant 2a. Phases of the atomic orbitals are shown for $k=(1/2,0,0)\pi/a$. All orbitals in each yz plane have the same phase, but the phase changes by $\exp(\pm i\pi/2)=\pm i$ for each translation $\pm a$ along the x direction in the crystal. The four orbitals on neighboring atoms in the yz plane form bonding $pp\pi$ interactions with the central atom. Interactions made by other neighboring orbitals with the central orbital cancel for $k=(1/2,0,0)\pi/a$.

consequently, they will be referred to as s, p_x, ..., d_{xy}, ..., functions, as though they were simple atomic orbitals.

The interactions which cause hybridization are represented by two-center integrals, $sp\sigma$, $sd\sigma$, $pd\sigma$, $pd\pi$, similar to those which describe interactions between like orbitals. Interactions between unlike orbitals occur only when their spatial symmetry properties are appropriate for the momentum of the crystal wave function, and the resulting effects are important only when bands derived from the unperturbed states have approximately equal energies. Thus, s functions interact with p_x functions when both have momenta $(0<|k|<\pi/a)$ along the [1,0,0] direction of a cubic crystal, but not when their momenta are in the [0,1,0] or [0,0,1] directions. Hybridization of s and p_x functions can be represented schematically for a face-centered-cubic crystal as follows: The unperturbed s states form crystal wave functions which have the configuration shown in Fig. 9 for $k=(1/2,0,0)\pi/a$. Similarly, the unperturbed p_x function has the configuration shown in Fig. 10 for the same value of momentum. The energies, E_s and E_p, of these crystal wave functions can be calculated by summing interactions between the central atom and its nearest neighbors, as was done previously for the simple cubic lattice. The results are available, for a general point of the Brillouin zone, in Table III of the article by Slater and Koster (13):

$$E_s=s_o+4ss\sigma(\cos\xi\cos\eta+\cos\xi\cos\zeta+\cos\eta\cos\zeta)$$

$$E_p=p_o+2pp\sigma(\cos\xi\cos\eta+\cos\xi\cos\zeta)$$
$$+2pp\pi(\cos\xi\cos\eta+\cos\xi\cos\zeta+2\cos\eta\cos\zeta),$$

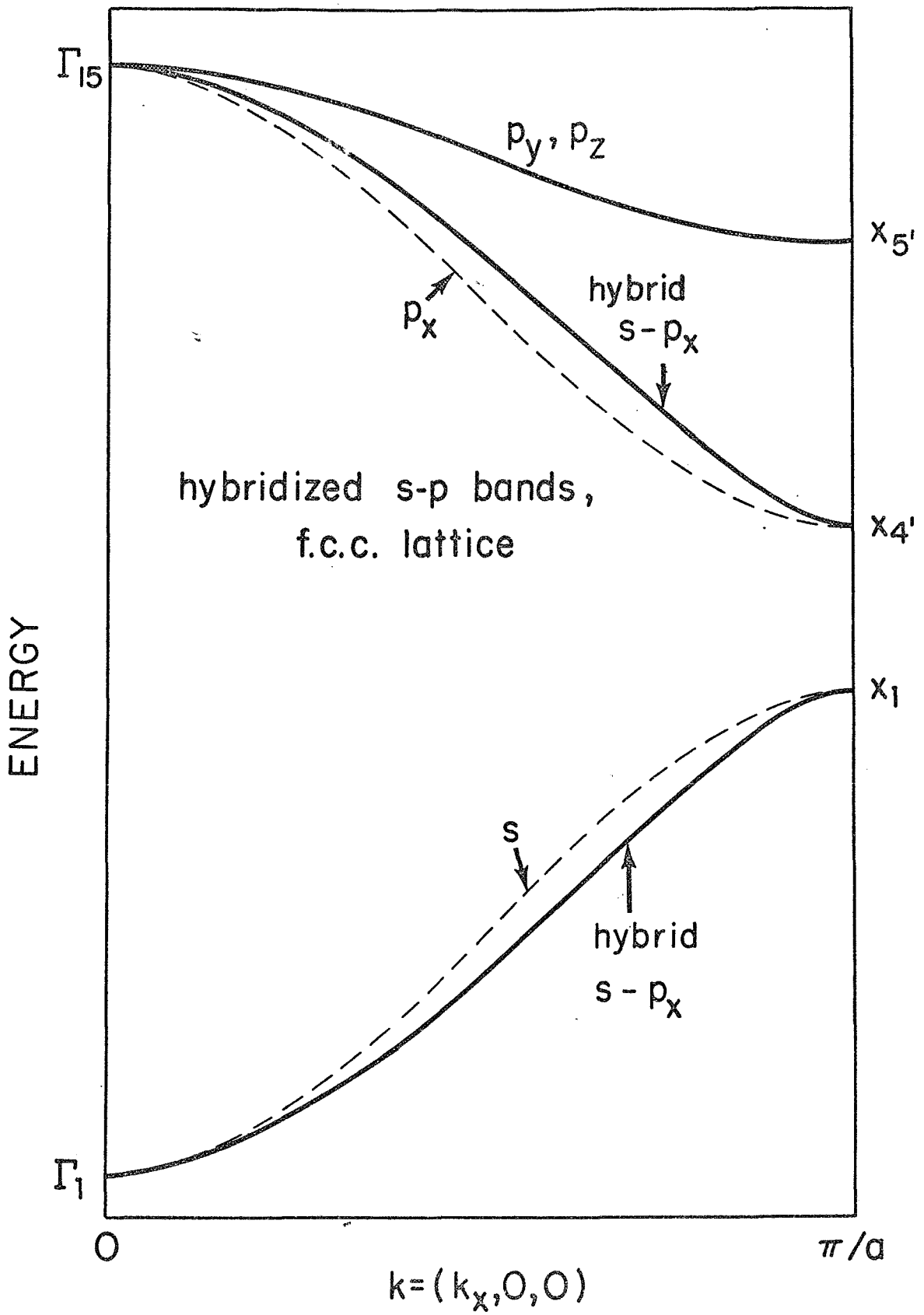

Fig. 11. - Electronic energy bands along the direction $k=(k_x,0,0)$ in the Brillouin zone of a face-centered-cubic crystal with lattice constant 2a. Atomic s and p_x functions mix to form hybrid crystal wave functions. Energies of these hybrid functions are displaced from the energies of crystal wave functions formed from pure s and pure p_x atomic orbitals by amounts determined by the degree of mixing. p_y and p_z functions do not mix with s functions along this direction in the Brillouin zone, but they do in crystal wave functions that have momenta along the directions of their respective principal axes.

where $\xi=ak_x$, $\eta=ak_y$, $\xi=ak_z$ and s_o and p_o are approximately the energies of the atomic s and p states. Energy bands calculated in this way for momenta along $k=(k_x,0,0)$ are shown by the dashed lines in Fig. 11.

When hybridization of these states occurs, the wave functions contain both s and p_x components, with the p-component carrying a phase factor $\exp(\pm\pi/2)=\pm i$ relative to the s component. The p_x component of the wave function on the central atom interacts with the s component of the wave function on surrounding atoms in one of the two ways shown in Fig. 12 (a) or (b). The bonding $sp\sigma$ interactions in (a) occur in the band of lower energy and depress its energy at $k=(1/2,0,0)\pi/a$ by $(8/\sqrt{2})sp\sigma$ times the product of the amplitudes of the s and p_x functions, whereas the antibonding interactions in (b) occur in the band of higher energy and raise its energy by the same amount.

Since both hybrid states contain s and p_x components, calculation of their energies proceeds by solving simultaneous equations for the energy, E, of each state:

$$(H_{ss}-E)a_{1s}+H_{sp}a_{1p}=0$$

$$H_{ps}a_{2p}+(H_{pp}-E)a_{2p}=0,$$

in which a_{1s} and a_{1p} are the amplitudes of the s and p_x functions, respectively, in one hybrid crystal wave function, and a_{2s}, a_{2p} are their amplitudes in the other. The matrix component of energy H_{ss} is simply the sum of interactions between an s function on the central atom and s functions on neighboring atoms, whereas H_{sp} is the sum of interactions between an s function on the central atom

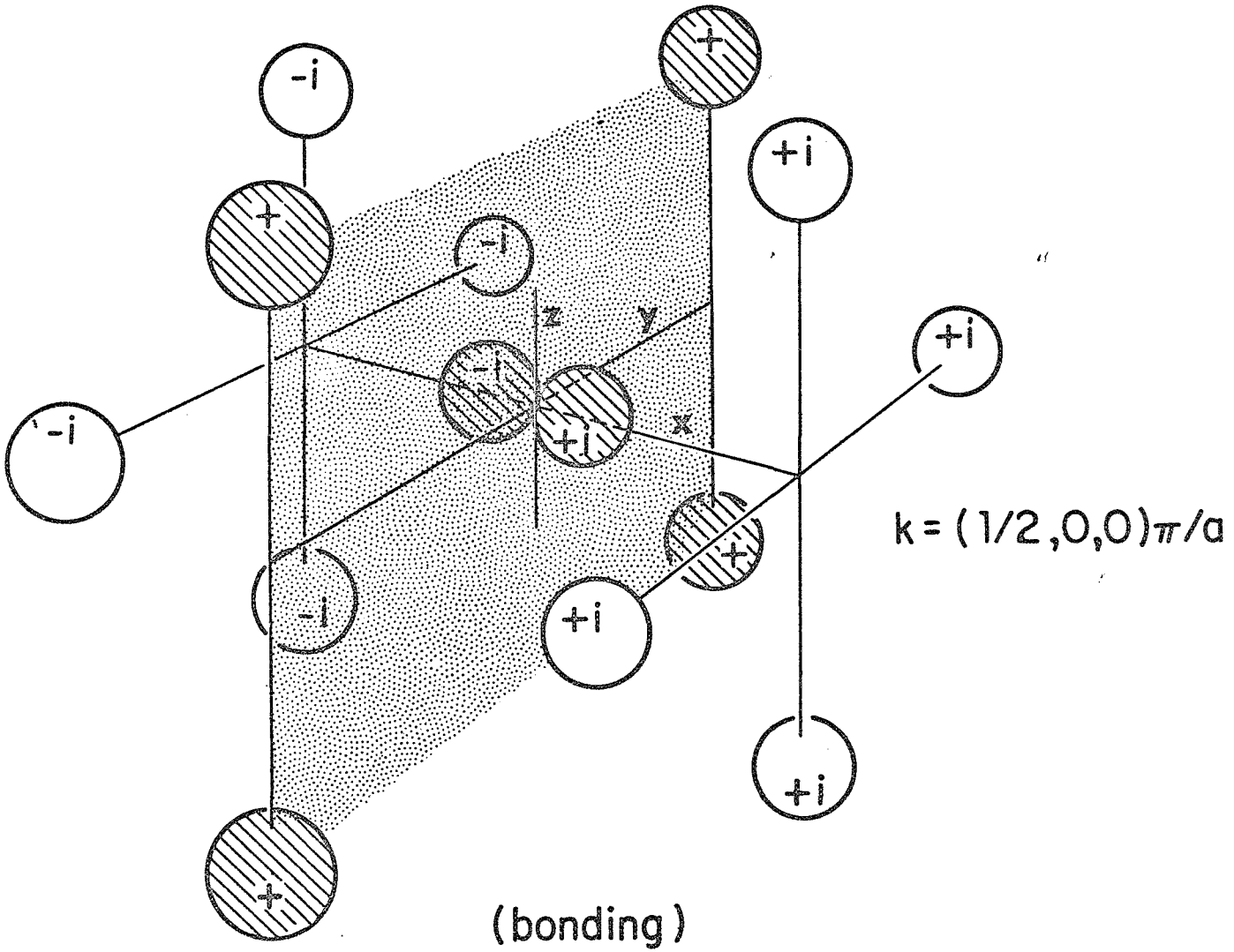

Fig. 12(a) - Bonding interactions at k=(1/2,0,0)π/a between components of s-p_x hybrid crystal wave functions in a face-centered-cubic crystal with lattice constant 2a.

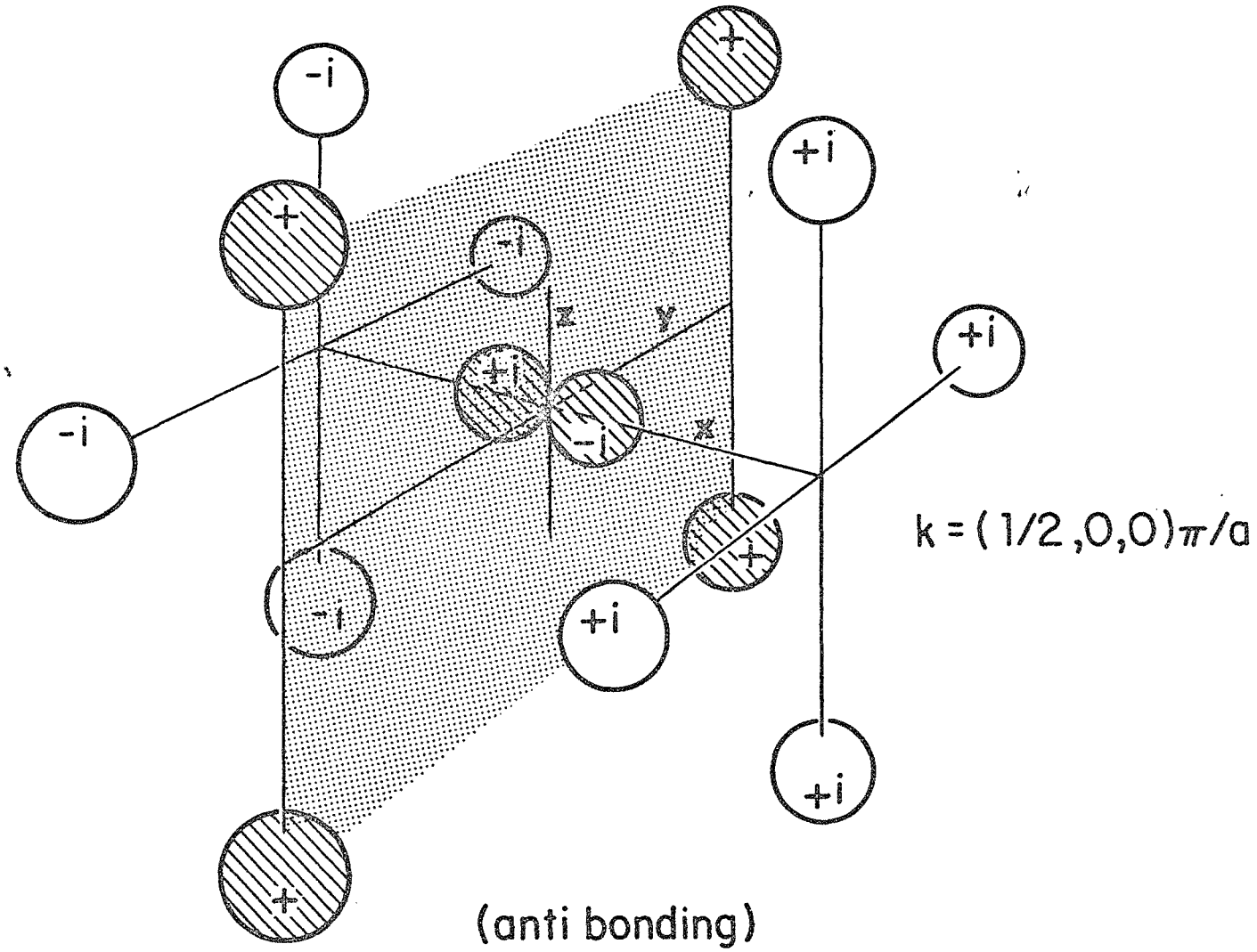

Fig. 12(b) - Antibonding interactions at k=(1/2,0,0)π/a between components of s-p_x hybrid crystal wave functions in a face-centered-cubic crystal with lattice constant 2a.

and p_x functions on its neighbors. $H_{ps}(=H_{sp})$ and H_{pp} are the corresponding sums for a p_x function on the central atom. These sums (matrix components of energy) are tabulated for cubic crystals in Table III of the article by Slater and Koster (13). Miasek (23) has listed the appropriate sums for hexagonal crystals also.

Energy bands calculated in this way for hybrid s-p_x bands are shown for momenta along $k=(k_x,0,0)$ by the solid lines in Fig. 11. The p_y and p_z functions do not mix with s functions along this direction in the Brillouin zone.

Hybridization does not affect the cohesive energy so long as both of the states which interact are occupied by electrons, since equal numbers of states are raised or lowered by equal amounts. If the states of higher energy are vacant, however, hybridization increases the cohesion by causing an uncompensated increase in the bonding of lower states. Such an effect is illustrated in the hybrid s-p_x bands of Fig. 11. If the number of electrons per atom is less than two, states of the lower band only are occupied and hybridization increases cohesion by increasing the strength of bonding of electrons in the lower band. If the Fermi level lies above the top of the p band at Γ_{15}, however, both the s and p bands are occupied and no net change in cohesion results from the s-p hybridization because the increased bonding of the lower states is cancelled exactly by weakened bonding in the upper states.

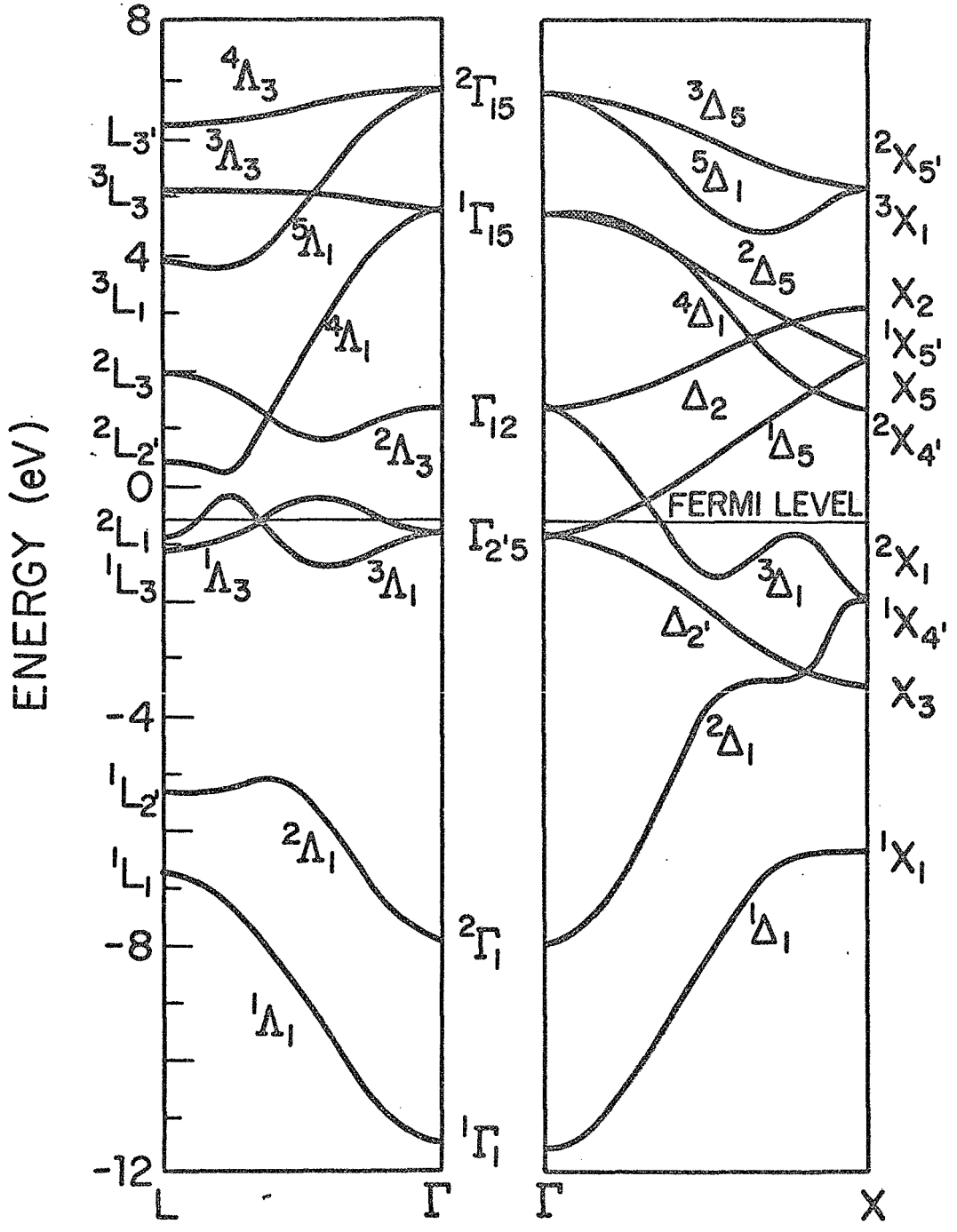

Fig. 13. - Energy bands along two directions of high symmetry, Δ and Λ, in the Brillouin zone of TiC, calculated using the simplified LCAO method of Slater and Koster (Ref. 10). Δ designates points in the fcc Brillouin zone on the line from Γ (k=0) to X (k=(1,0,0)π/a). Λ designates points on the line from Γ to L (k=(1/2,1/2,1/2)π/a). [From R. G. Lye and E. M. Logothetis, Phys. Rev. 147, 622 (1966).]

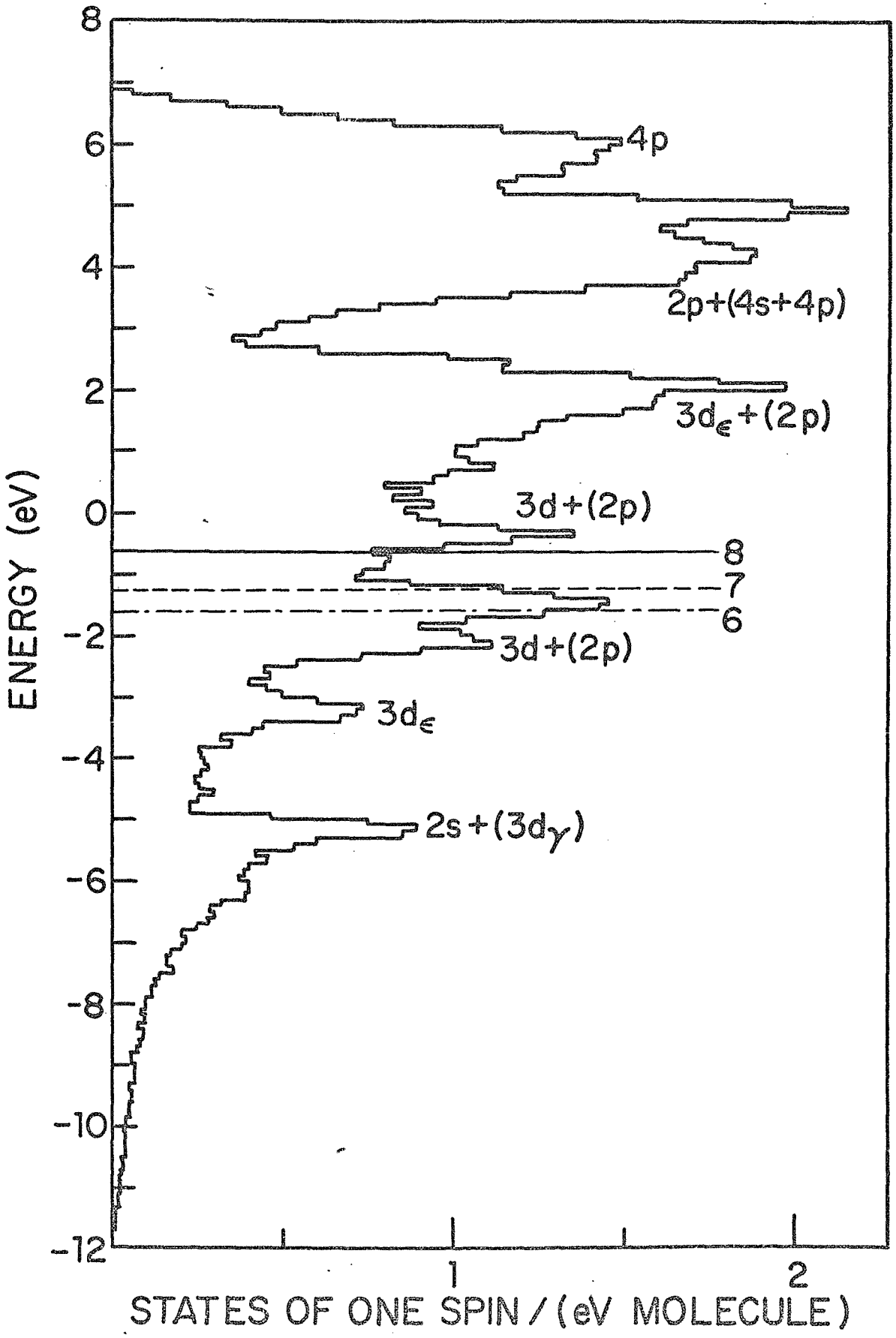

Fig. 14. - Density-of-states histogram for TiC derived from the band structure of Fig. 13. Fermi levels are indicated for six, seven, and eight electrons respectively. [From R. G. Lye and E. M. Logothetis, Phys. Rev., 147, 622 (1966).]

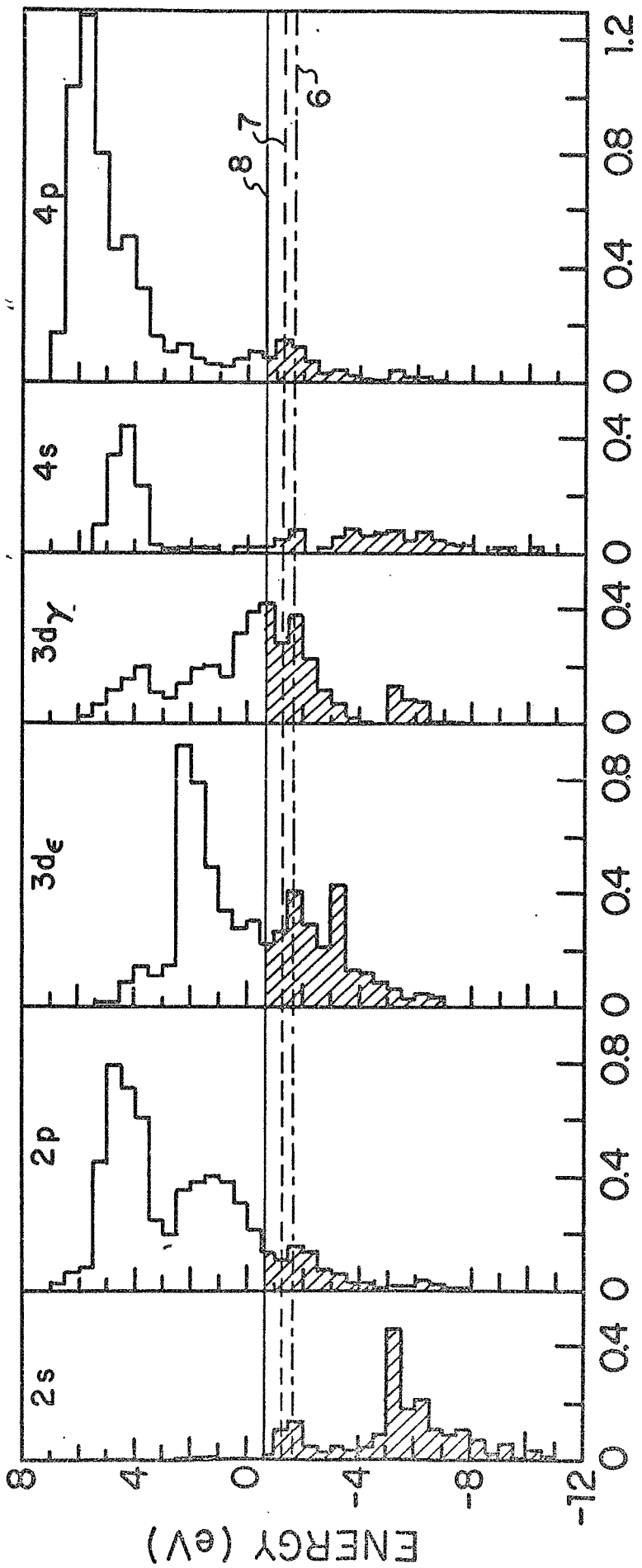

Fig. 15. - Density-of-states histograms for the separate atomic states from which the band structure of Fig. 13 was calculated. [From R. G. Lye and E. M. Logothetis, Phys. Rev., 147, 622 (1966).]

III. Band Structure of Titanium Carbide.

The energy band structure of TiC was calculated by Lye (17) according to the approach outlined in Section II but using, in addition, the further simplification suggested by Slater (13): Instead of attempting tedious and uncertain calculations of values for the two-center integrals, these integrals were used as adjustable parameters which were varied to make the computed band structure agree with experimental data. Measurements of the near-normal-incidence reflectivity (17) provided energies of prominent optical transitions to which the calculated band energies had to be adjusted. Other information was provided by studies of the energy dependence of photoemission (17), and by measurements of the Hall coefficient (24,25) resistivity (24), piezoresistance (26), and thermoelectric power (27).

The energy band structure obtained by this method is shown in Fig. 13 for directions in the Brillouin zone from the center, Γ, to boundary points X and L at $(1,0,0)\pi/a$ and $(1/2,1/2,1/2)\pi/a$ respectively. A total density-of-states curve obtained from the same calculation is shown in Fig. 14, and individual density-of-states curves are shown in Fig. 15 for the atomic states from which the crystal wave functions were derived.

The energy band structure determined by this method differs from that obtained by Bilz (12), shown in Fig. 16, in two important respects. First, the 2p bands of carbon, which are labeled Γ_{15} at the center of the Brillouin zone lie 8 eV above the energy calculated by Bilz. Second, as indicated also in the density-of-states curve of Fig. 15, the d band is far broader than that computed by Bilz.

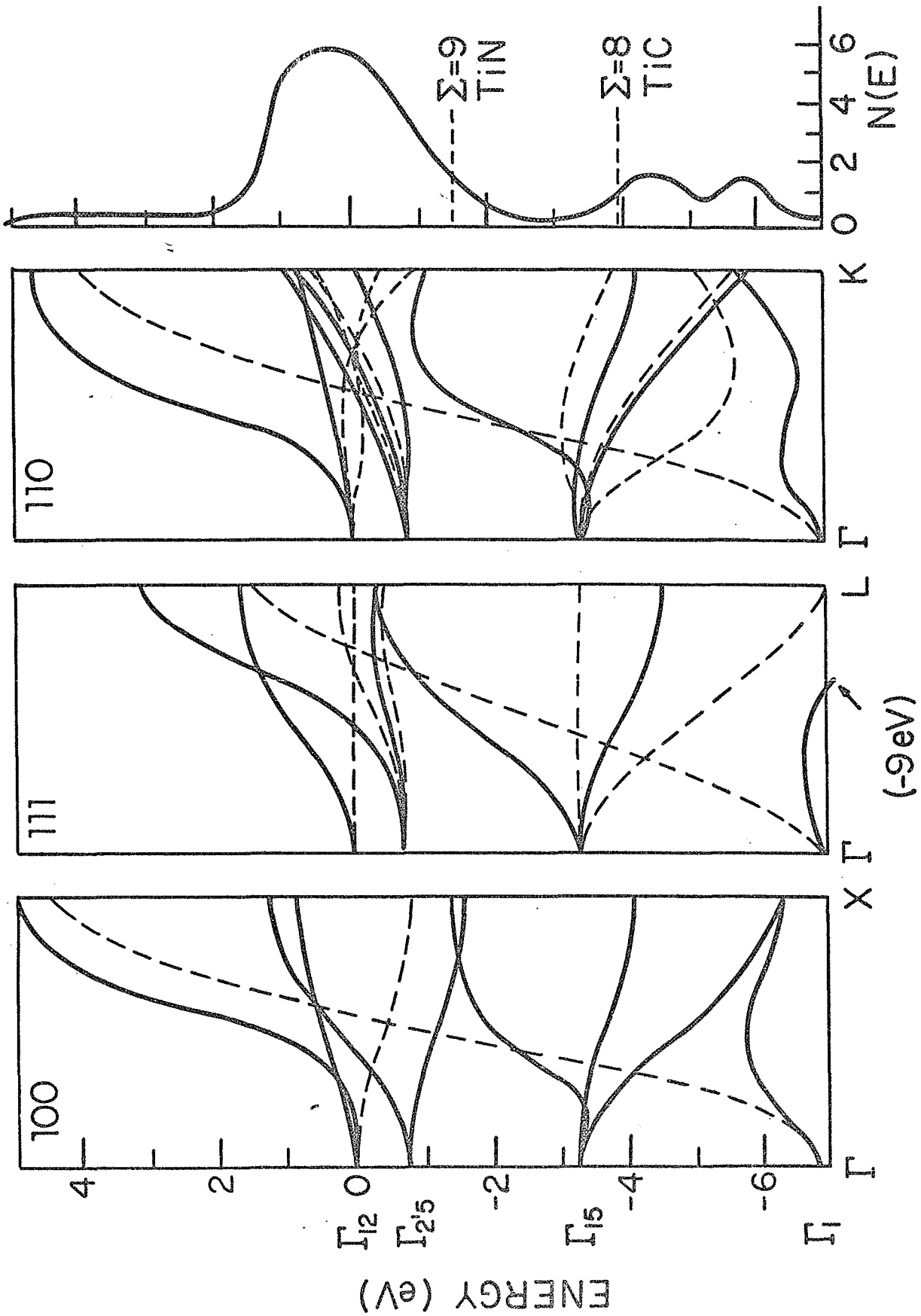

Fig. 16. - Band structure of a (hypothetical) titanium hard metal with the rocksalt crystal structure. [From H. Bilz, Z. Physik, 153, 338 (1958).]

Elevation of the 2p states is a consequence of several effects. Part of this elevation, 4 eV, results simply from using the energy of the atomic p state of carbon instead of the averaged value of carbon, nitrogen, and oxygen adopted by Bilz. The fact that pronounced changes in the band structure result from the use of a different value for this energy demonstrates that no single energy band structure can be used to represent, with useful accuracy, the three compounds, TiC, TiN, and TiO.

Further elevation of the 2p states (1.5 eV) results from the use of $pp\sigma$ interactions between carbon 2p orbitals somewhat stronger than those employed by Bilz. The modification can be justified in the same way as is done later for the 3d-3d interactions in the discussion of the breadth of the d-band.

Titanium 4p-wave functions, which were not considered by Bilz, interact with the carbon 2p states and lower their energy at the center of the Brillouin zone, Γ, by approximately 0.4 eV. An additional elevation of 2.77 eV is necessary, therefore, to account for the optical properties of TiC, and a similar displacement is required for the carbon 2s states. If this remaining elevation of carbon states relative to the titanium states is attributed solely to electrostatic effects determined by the Madelung potential difference, $2\alpha ze^2/a$ (28,16), it corresponds to a charge transfer of approximately 0.15 electrons from carbon to titanium atoms. The magnitude of the charge transfer needs to be determined more precisely, but the present estimate indicates that ionic bonding contributes only a small fraction ($\sim$ 1%) of the total cohesive energy, 327 kcal/mole calculated from thermodynamic properties (29-31).

Broadening of the d-band may be explained on the basis of work by Costa and Conte (14). They showed that d-d interactions between metal atoms are strengthened markedly by the potential of carbon atoms in the octahedral interstices of the fcc titanium sublattice. By similar arguments, it is expected that other metal-metal and carbon-carbon interactions may be somewhat stronger than the values suggested by Bilz.

As a result of the strong d-d interactions, bonding states of the d-band are depressed in TiC to energies lower than they would have in (hypothetical) fcc titanium, or in normal hcp titanium metal. The presence of these low-lying d states contributes greatly to the total cohesion. Sufficient numbers of the states are available to accept not only the 3d electrons originally on the titanium atom, but also some of the 4s electrons of titanium and some of the 2p electrons of carbon. The density-of-states curves of Fig. 15 indicate that the electronic configurations of the atoms in TiC are approximately $(2s)^2(2p)^{3/4}$ for carbon, and $(3d)^4(4s)^{3/4}(4p)^{1/2}$ for titanium. Since the isolated atoms have the configurations $(2s)^2(2p)^2$ and $(3d)^2(4s)^2$, it appears that approximately 1 1/4 electrons have been transferred from carbon 2p states to levels derived from titanium atomic states. The net charge transfer, however, is less than this amount because the metal wave functions overlap again onto the carbon atom sites.

IV. Bonding in Titanium Carbide.

Although the calculated band structure is tentative and subject to considerable refinement by more precise methods of analysis, it may be used to provide a preliminary interpretation of the bonding in titanium carbide. A qualitative description of the bonding may be obtained by considering the amplitudes and interactions of atomic functions present in the computed crystal wave functions associated with occupied electronic states. Wave functions have been examined in this way for points in the Brillouin zone along the directions Γ-X and Γ-L in the energy bands of Fig. 13. The results suggest the possibility of constructing equivalent orbitals in the manner proposed by Hall (1) and Slater (2). For the present, however, only contributions to bonding from individual atomic and simple hybrid orbitals will be described.

It will be noted that carbon 2s states contribute little to the bonding; they are almost completely occupied (Fig. 15) and, consequently, contribute almost as many antibonding as bonding interactions. The bonding they do contribute results primarily from effects of hybridization with carbon 2p states near $k=(1/2,0,0)\pi/a$ and with metal 3d, 4s, and 4p states near the Brillouin zone boundaries.

The titanium 3d electrons contribute to the bonding through simple d-d interactions and through s-d and p-d hybridization. The effects of such hybridization may be illustrated by considering first the simple d-d interactions.

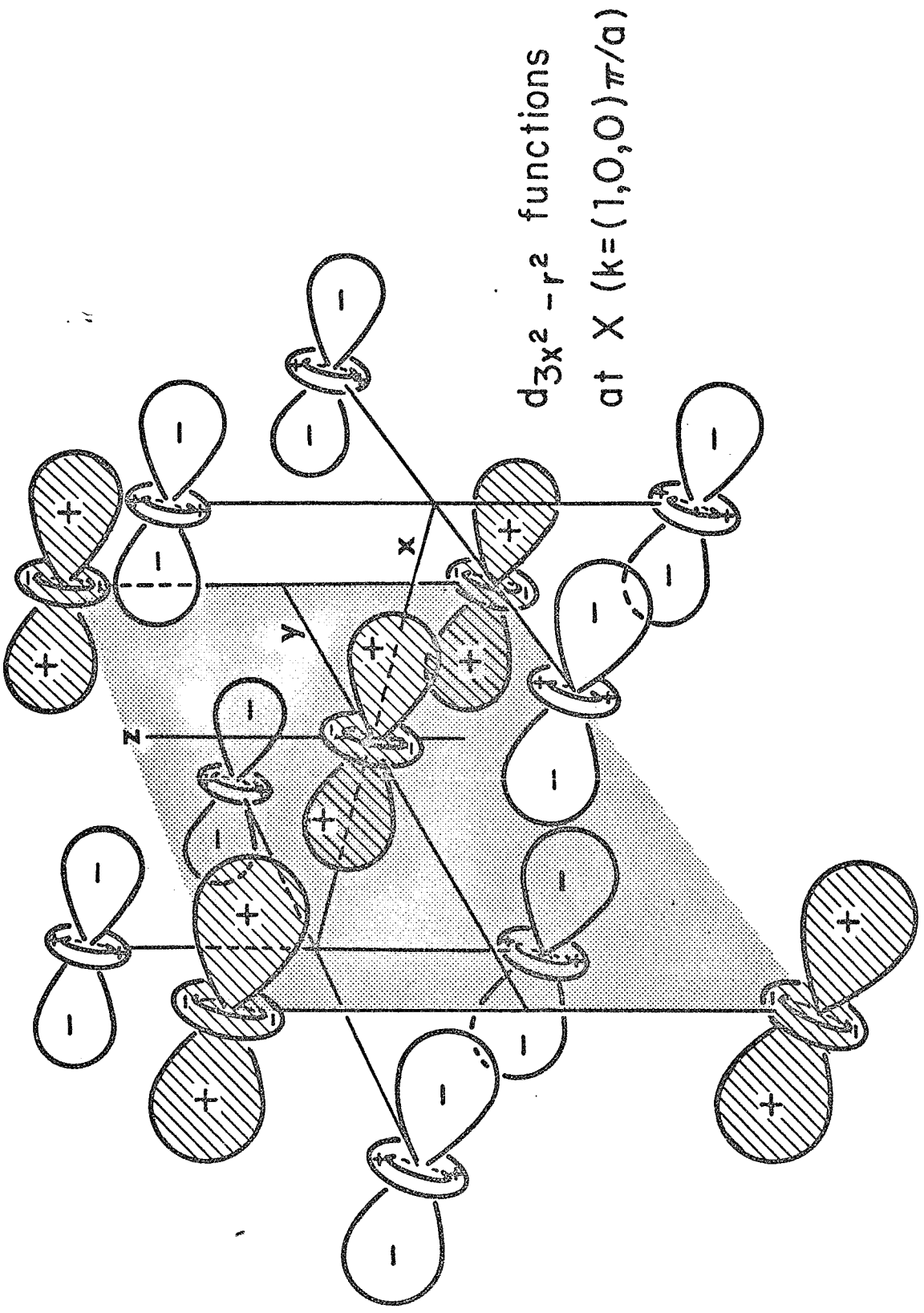

Fig. 17. - Bonding interactions between d_γ orbitals, with symmetry $3x^2-r^2$, at the Brillouin zone boundary $k=(1,0,0)\pi/a$ of TiC (lattice constant 2a). The four orbitals in the y-z plane each form 1/4 $dd\sigma$+3/4 $dd\delta$ bonding interactions with the central orbital. The eight orbitals at $(\pm a,\pm a,0)$ and $(\pm a,0,\pm a)$ each form 3/4 $dd\pi$ bonding interactions and 1/16 $dd\sigma$+3/16 $dd\delta$ antibonding interactions. Most of the bonding is provided by the $dd\pi$ contributions.

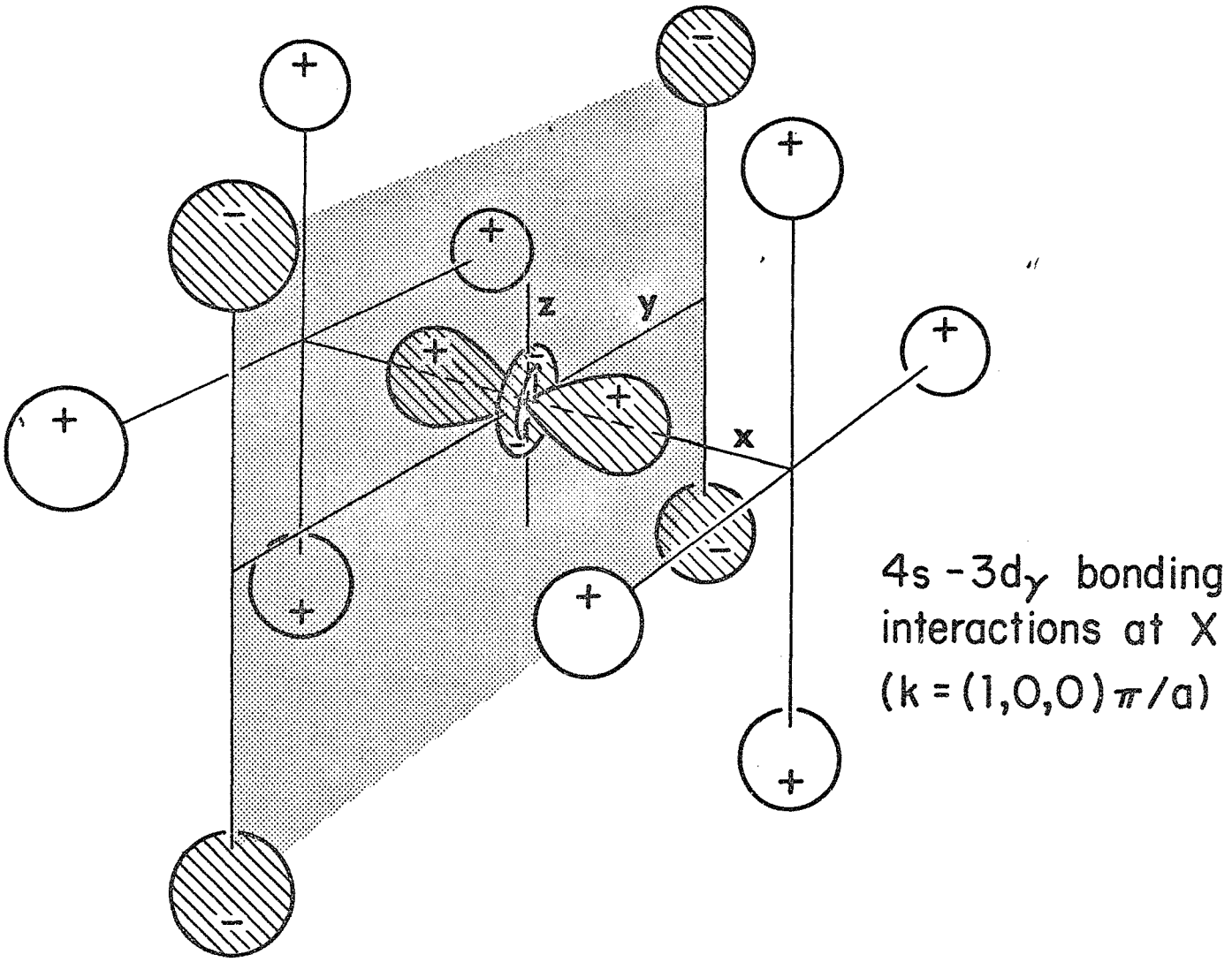

Fig. 18. Bonding interactions at k=(1,0,0)π/a between components of 4s-3d$_\gamma$ hybrid crystal wave functions in TiC (lattice constant 2a).

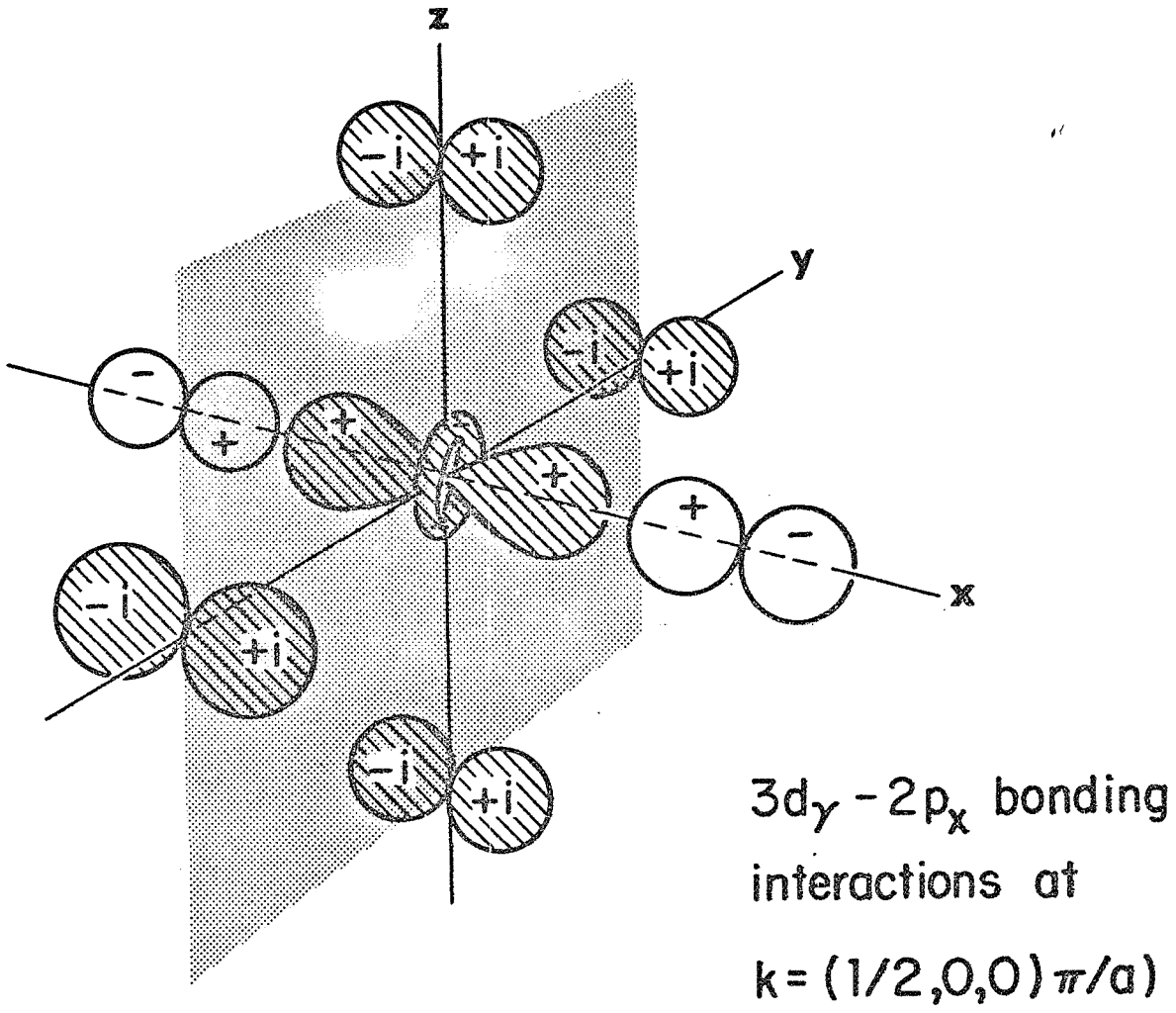

Fig. 19. Bonding interactions at k=(1/2,0,0)π/a between components of $3d_\gamma$-$2p_x$ hybrid crystal wave function in TiC (lattice constant 2a).

One of the major contributions to d-band bonding arises from interactions near the Brillouin zone boundary at X ($k=(1,0,0)\pi/a$) between $3d_\gamma$ orbitals with $3x^2-r^2$ symmetry*. Their configuration at X is illustrated in Fig. 17. The $dd\pi$ component of interaction between the orbitals at $(\pm a,\pm a,0)$ and $(\pm a,0,\pm a)$ and the central orbital provides most of the bonding near X, but leads to a net antibonding interaction at Γ_{12}. These $3d_\gamma$ orbitals hybridize with 4s orbitals near X, thereby increasing the cohesion because the upper hybrid states are vacant. The energy of $3d_\gamma$-4s hybrid states is lowered through interactions like those shown in Fig. 18 for $k=(1,0,0)\pi/a$.

In addition, the $3d_\gamma$ states are depressed near $k=(1/2,0,0)\pi/a$ as a result of interactions with carbon $2p_x$ states, as shown in Fig. 19. Such interactions contribute to metal-carbon bonding and further increase the cohesion since the upper hybrid states again are largely unoccupied. Although considerable hybridization of these states occurs with carbon 2s states also, no net change in cohesion results because both hybridized states are occupied. Energy levels associated with these states fall in the bands labeled $^1\Delta_1$, $^2\Delta_1$, and $^3\Delta_1$ in Fig. 13.

Very similar interactions occur along the (1,1,1) direction in the Brillouin zone with 3d orbitals formed from linear combinations of d_ϵ wave functions. The resulting orbitals have the same shape as those illustrated in Fig. 17 but have their principal axes directed along body diagonals in the

---

*The d functions form two groups in a cubic crystal, the three d_ϵ functions, which have symmetry xy, yz, and zx; and the two d_γ functions, which have symmetry $3x^2-r^2$ and z^2-y^2. Orbitals with d_ϵ symmetry form wave functions in the state $\Gamma_{25'}$ (Fig. 13), those with d_γ symmetry form wave functions in the state Γ_{12}. Atomic orbitals with s, p, and d symmetries are illustrated in Fig. 9 of Ref. 22.

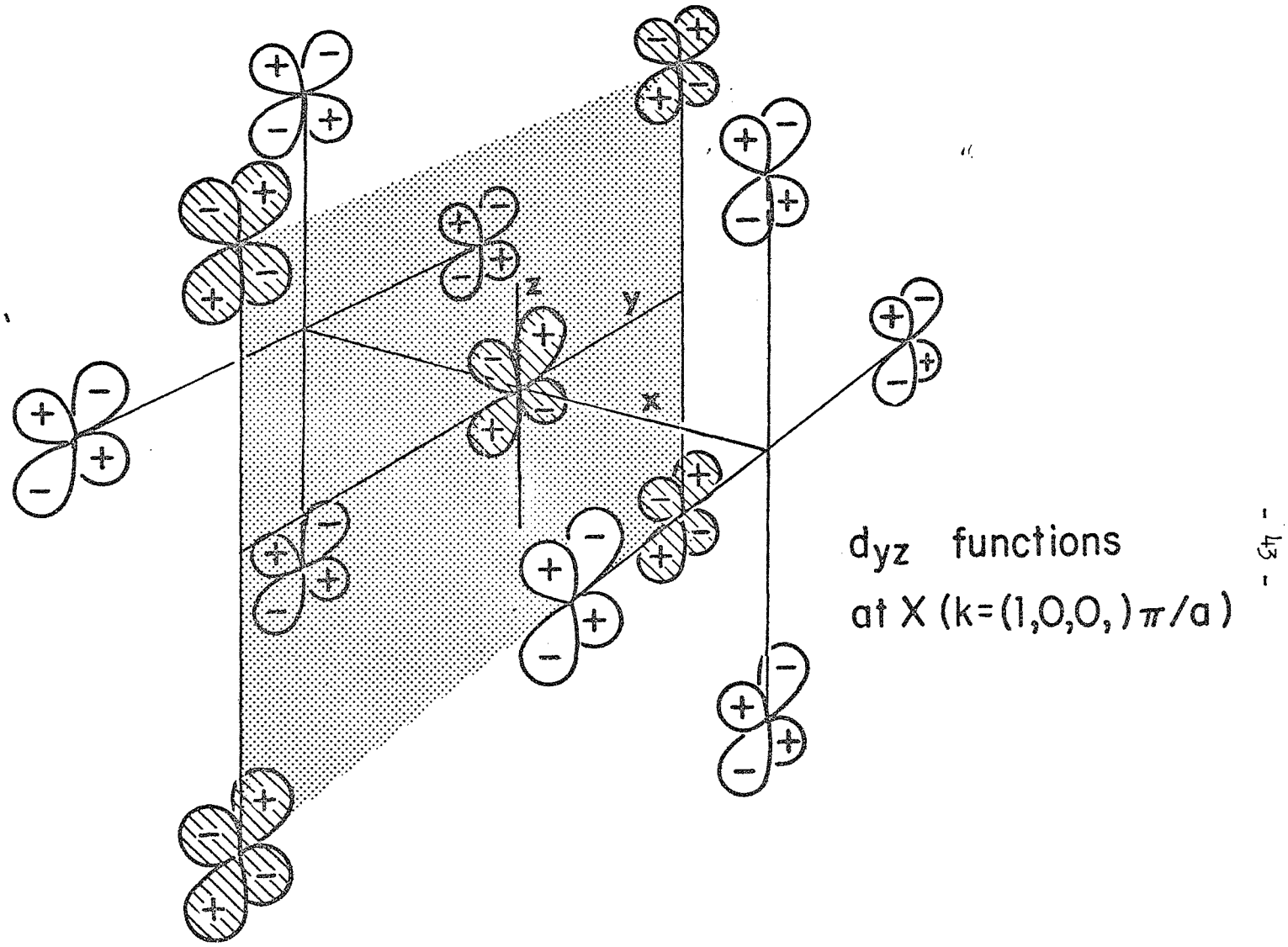

Fig. 20. - Bonding interactions between d_ϵ orbitals, with symmetry yz, at the Brillouin zone boundary $k=(1,0,0)\pi/a$ of TiC (lattice constant 2a). The four orbitals in the y-z plane each form 3/4 $dd\sigma$+1/4 $dd\delta$ bonding interactions with the central orbital. The eight orbitals at $(\pm a,\pm a,0)$ and $(\pm a,0,\pm a)$ each form 1/2 $dd\pi$ bonding interactions and 1/2 $dd\delta$ antibonding interactions.

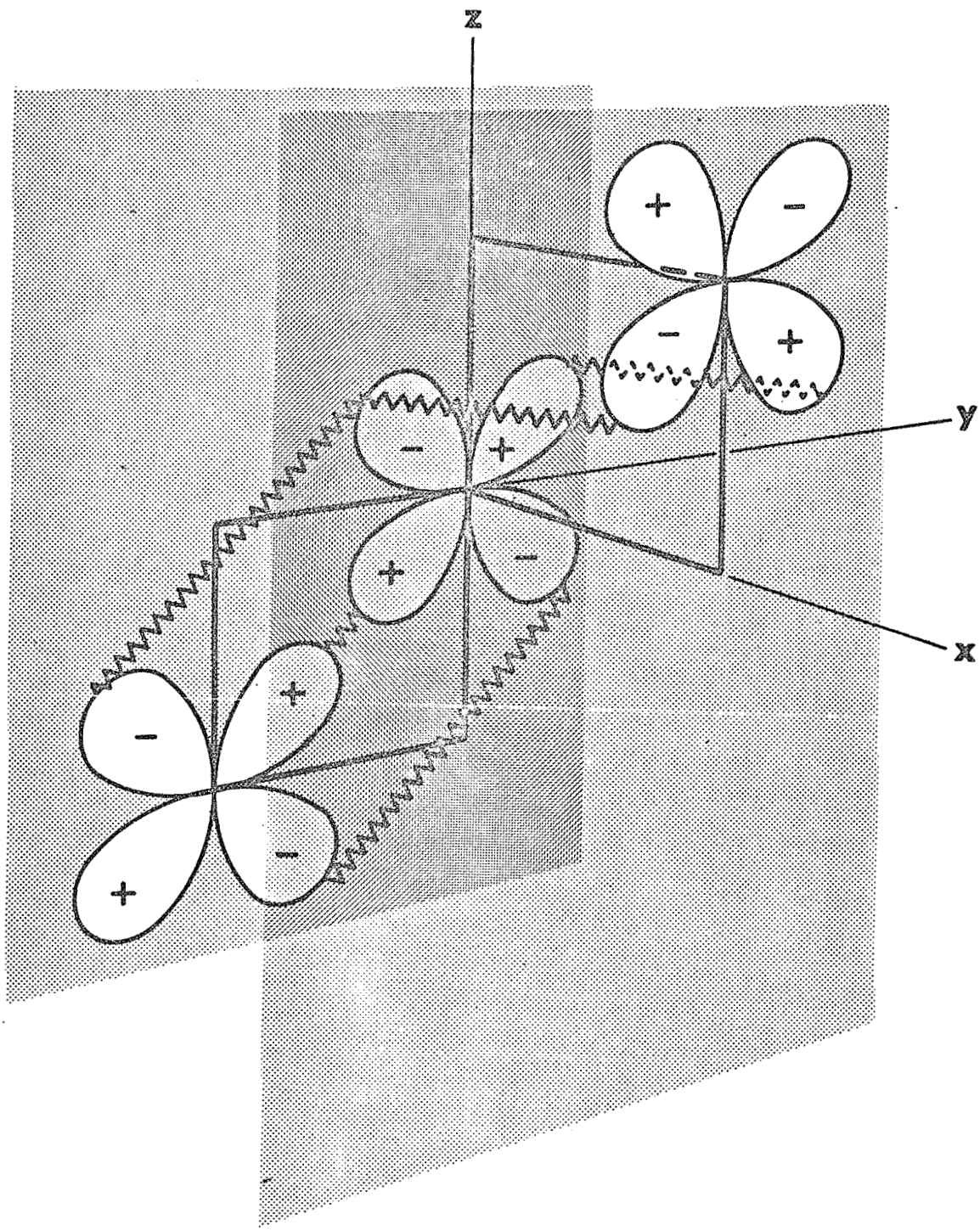

Fig. 21. - Isolated view of the d_{yz} orbitals at (0,0,0), (a,0,a), and (0,-a,-a) in Fig. 20.

crystal. Interactions between them are strongly bonding, and again, they hybridize with 4s and 2p orbitals to increase the bonding further. Energy levels for these states fall in the bands $^1\Lambda_1$, $^2\Lambda_1$, and $^3\Lambda_1$.

Additional d-band bonding arises along the (1,0,0) direction of the Brillouin zone from interactions between d_ϵ orbitals with yz symmetry. The strongly bonding configuration at the zone boundary X ($k=(1,0,0)\pi/a$) is illustrated in Fig. 20. The central orbital and the orbitals at $(0,\pm a,\pm a)$ contribute a strong component of $dd\sigma$ bonding and a weak component of $dd\delta$ bonding, whereas the orbitals at $(\pm a,\pm a,0)$ and $(\pm a,0,\pm a)$ contribute strong $dd\pi$ bonding and weak $dd\delta$ antibonding interactions. The bonding of orbitals at (0,-a,-a) and (a,0,a) with the orbital at (0,0,0) is emphasized in Fig. 21. These orbitals do not interact with 4s, 2s or 2p orbitals along the (1,0,0) direction in the Brillouin zone. Energy levels associated with these orbitals lie in the band $\Delta_{2'}$.

Additional metal-metal bonding is contributed by the 4s orbitals in crystal wave functions with momenta near k=0. Although considerable hybridization occurs between 4s and 2s orbitals, little net change in cohesion results from the mixing because both hybrid states are occupied near the center of the zone.

A small component of metal-metal bonding is contributed also by the 4p orbitals of titanium, which are unoccupied in the free atom but become occupied near the zone boundaries in the solid. The 4p orbitals are occupied, however, only in hybrid wave functions in which they are a minor

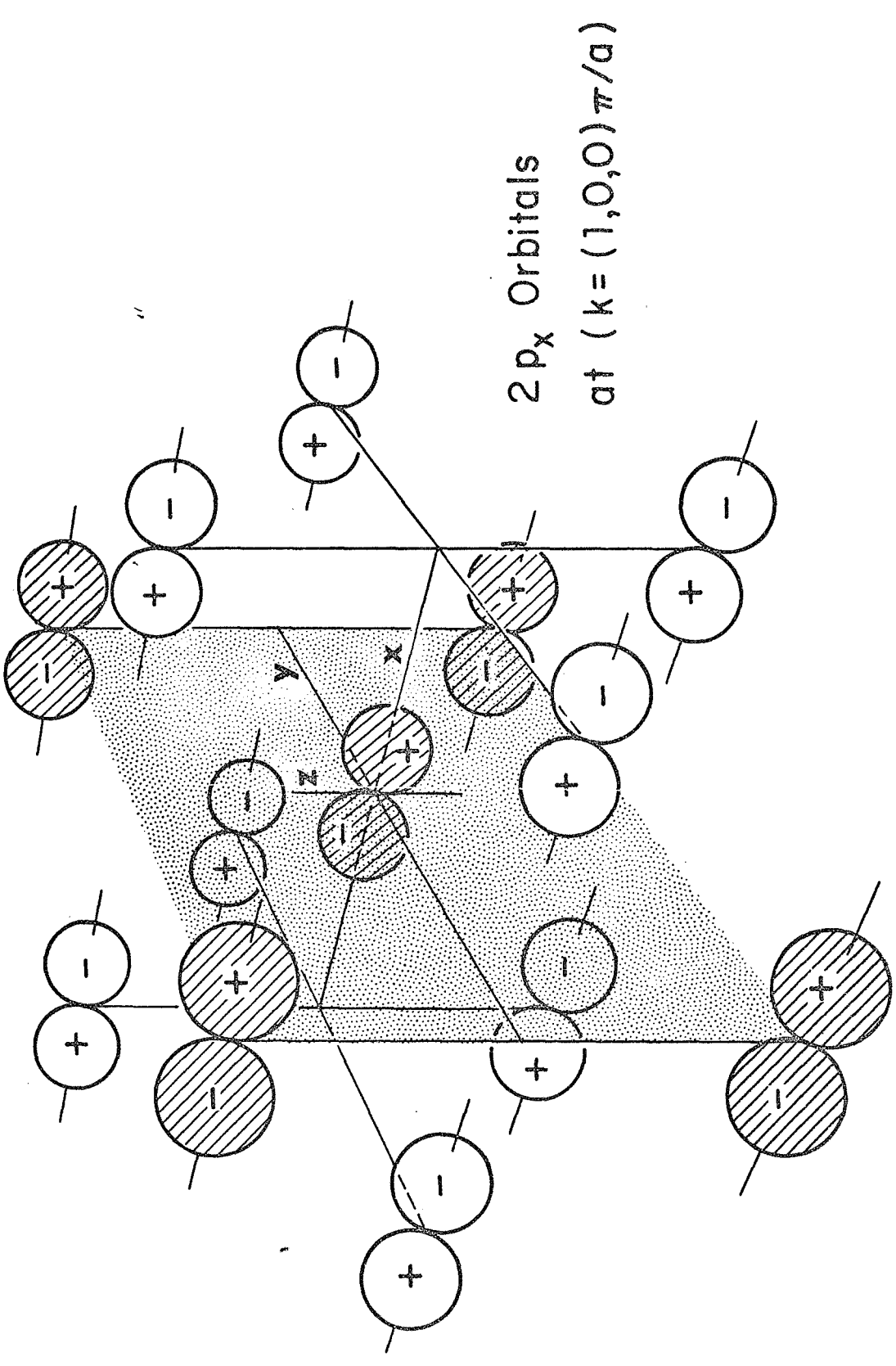

Fig. 22. - Bonding interactions at k=(1,0,0)π/a between $2p_x$ orbitals in TiC (lattice constant 2a).

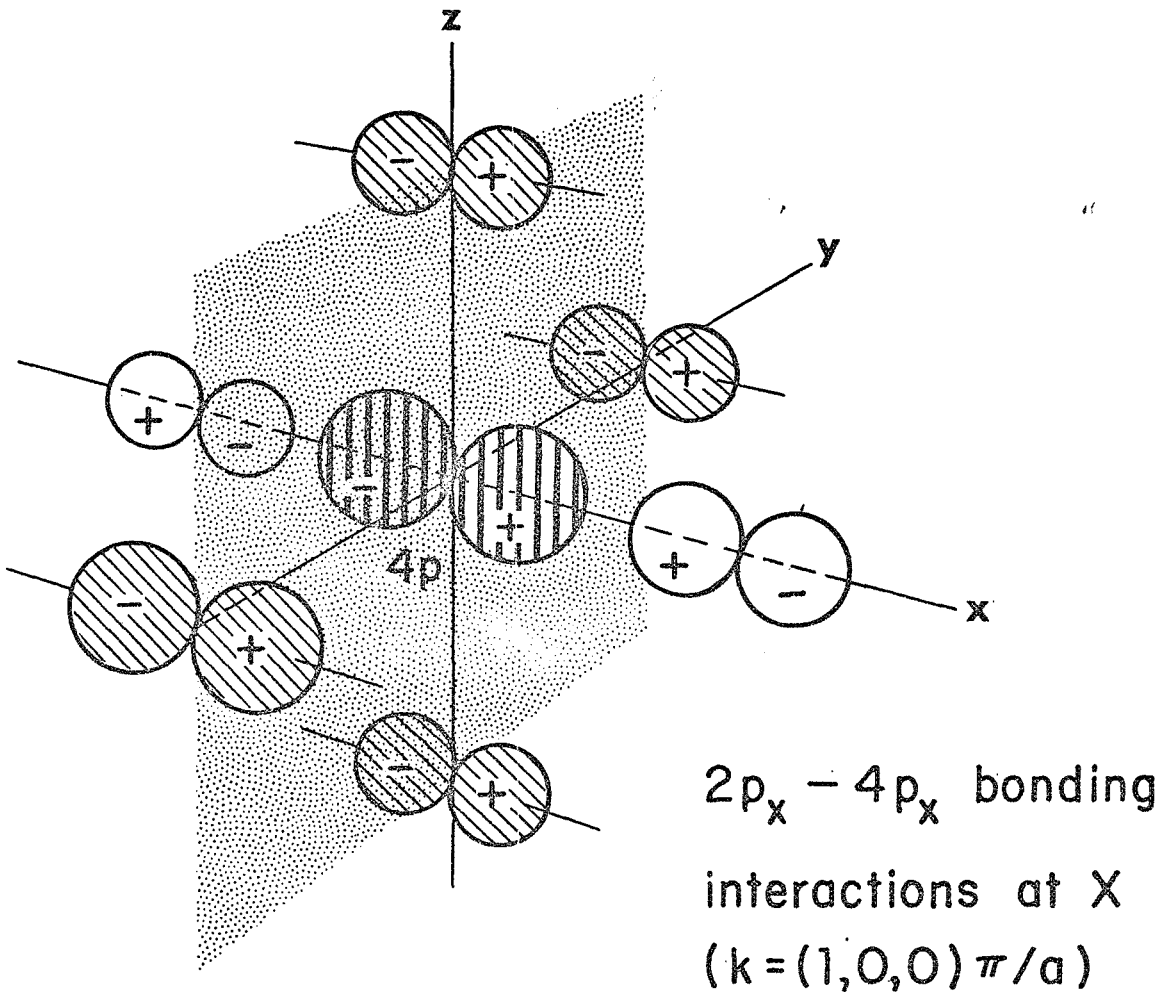

Fig. 23. - Bonding interactions at k=(1,0,0)π/a between components of $2p_x$-$4p_x$ hybrid crystal wave functions in TiC (lattice constant 2a); $4p_x$ orbital on central titanium atom, $2p_x$ orbitals on neighboring carbon atoms.

component. Their contribution to the bonding may be illustrated through the influence they exert on the more important carbon-carbon bonding of 2p orbitals.

Strong carbon-carbon bonding is contributed by 2p orbitals in small regions of the Brillouin zone near the boundaries at X and L. A strongly bonding configuration is shown in Fig. 22 for $2p_x$ orbitals with momenta near X ($k=(1,0,0)\pi/a$). Metal $4p_x$ orbitals contribute similar, but weaker, metal-metal bonding interactions. In addition, however, they hybridize with carbon $2p_x$ orbitals and increase the cohesion through the resulting carbon-metal interactions since the lower hybrid states only are occupied. The bonding $2p_x$-$4p_x$ interaction is shown in Fig. 23. Occupied 2p and 4p states thus contribute carbon-carbon, metal-metal, and carbon-metal bonding interactions. Energy levels belonging to these states lie primarily in the $^3\Delta_1$ band close to X.

Carbon 2p orbitals are occupied at the zone boundary near L also. The bonding orbitals have their lobes directed along body diagonals of the crystal and contribute strong carbon-carbon bonding interactions. They interact also with d_ϵ functions of symmetry xy+yz+zx (lobes directed along body diagonals) to increase further the carbon-metal bonding. Hybrid states associated with these 2p-3d interactions lie primarily in the bands $^1\Lambda_1$ and $^3\Lambda_1$ near L. Additional carbon-metal bonding is contributed by 2s-4p interactions in the band $^2\Lambda_1$ near L.

V. Discussion.

The bonding of TiC, as inferred from the empirical band structure discussed here, contains contributions from metal-metal, metal-carbon, carbon-carbon, and ionic interactions, and the composite nature of this bonding is reflected in its properties. Prominent metal-metal interactions, for example, cause many of the physical properties of TiC to be similar to those of the transition metals. It might be expected, therefore, that the properties of TiC would be closely related to those of its parent metal, titanium. In TiC, however, these metal-metal interactions are modified by two effects: (1) Metal-metal bond strengths are increased by the potential of carbon atoms in the region of overlap between metal orbitals, and (ii) the number of electrons participating in such bonds is increased by transfer of electrons from carbon to metal atomic orbitals.

This electron transfer would be expected to make TiC more like vanadium or chromium than titanium, but the enhanced metal-metal interactions probably increase its melting point and strength to values beyond those of the first series transition metals, in much the same way that stronger metal core potentials increase the bonding of heavier transition metals within each group. Thus, the metal-metal interactions alone would make TiC a strongly bonded substance similar to transition metals of the second series. Since the increased strength of the metal-metal bonds may also increase the covalent character intrinsic to interactions between partially occupied-orbitals, TiC would be

expected to have hardness and strength similar to those of the harder transition metals. The nature and magnitude of observed differences between TiC and these metals indicate, however, that the other contributions to bonding must also play a significant role. Although the ionic interactions may influence certain properties, they appear to contribute little to the bonding. Metal-carbon and carbon-carbon interactions, on the other hand, provide covalent components of bonding which together contribute substantially to the great hardness, brittleness, and high melting point exhibited by TiC.

The electrical conductivity and other typically metallic transport properties of TiC appear to arise primarily from the presence of a small conduction band near $\Gamma_{2'5}$ dervied from titanium $3d_\epsilon$ states rather than, as had been anticipated, from the overlapping bands that have substantially 4s character. Details of the band structure near the Fermi level are not clearly established, however, so that other electron and hole bands can not be excluded from consideration.

The band structure discussed here suggests that bonding in TiC is determined primarily by metal-metal interactions similar to those in the "hard" transition metals, with additional covalent bonding contributed by interactions involving carbon atoms. Thus, this method of analysis appears to substantiate the proposals made by Kiessling and Robins rather than that of Rundle.

This interpretation of the bonding in TiC from its band structure may be used as a basis for discussing the bonding in other cubic refractory hard metals also. TiN and TiO, for example, are expected to exhibit bonding properties that differ from those of TiC mostly because of differences in the energies

of the electronic states in their nonmetal atoms. Because the 2p atomic states of nitrogen lie 2.5 eV lower than the 2p states of carbon, their degree of hybridization with 3d and 4s states of titanium in TiN may be somewhat greater than in TiC, and the charge transfer between atoms may be smaller. Nitrogen-nitrogen and nitrogen-metal interactions, consequently, may contribute somewhat more to the bonding in TiN than do the corresponding interactions in TiC, whereas the ionic contribution is expected to be weaker. On the other hand, the more prominent bonding properties, which arise from metal-metal interactions, should be similar in the two compounds.

The 2p atomic states of oxygen are 5.2 eV lower than they are in carbon; thus, the 2p bands of TiO are expected to overlap the lower portion of the metal 3d bands. The large number of low-lying 2p states will permit the transfer of electrons from titanium to oxygen states, thereby decreasing the bonding due to d-d interactions. Conversely, oxygen-oxygen and titanium-oxygen bonding will be strengthened, both by the greater number of occupied 2p states, and by the greater degree of hybridization that will result from the proximity of the oxygen 2p and metal 3d and 4s bands. Although the charge transfer probably will be in the direction opposite to that in TiC, it may be substantially larger and so contribute an important fraction of the total cohesion in TiO.

It must be acknowledged that the discussion of bonding presented here has only qualitative justification. Ruedenberg (32) has discussed the closely related problem for molecules and has indicated some of the difficulties

and uncertainties in such descriptions of bonding. Despite the limitations of this method, it does serve to improve the understanding of materials with complex bonding, and it may be as useful for the transition metals themselves as for compounds such as the one discussed here. Goodenough (33) has discussed the magnetic properties of transition metals and alloys from a related point of view, but the origins of their diverse bonding characteristics remain somewhat obscure. It should be possible now to clarify certain aspects of this problem, since numerous studies have been made recently of electronic energy bands in transition metals. Information derived from such studies needs to be made available in a form useful to metallurgists who work with these materials. The close relationship between band structure and bonding, illustrated here for TiC, may provide additional physical insight of value for such purposes.

Acknowledgements

Some of the work described here was prepared first for a lecture course given at the University of Washington in the summer of 1966. The hospitality of Professor J. I. Mueller and the School of Mineral Engineering during that time is acknowledged with appreciation. Professor J. W. McClure of the University of Oregon generously gave assistance with certain aspects of the work. It is a pleasure to acknowledge also the invaluable advice and encouragement provided by Dr. A. R. C. Westwood and J. D. Venables of RIAS during the preparation of the manuscript. The author is grateful for financial support provided by the NASA Research Division, Code RRM, Materials Research Branch, under contract NASw-1290.

References

(1) G. G. Hall, Phil. Mag. 43, 338 (1952).

(2) J. C. Slater, in Encyclopedia of Physics, edited by S. Flugge, (Springer-Verlag, Berlin, 1956).

(3) P. Schwarzkopf and R. Kieffer, Refractory Hard Metals (The Macmillan Company, New York, 1963).

(4) R. Kieffer and F. Benesovsky, Hartstoffe (Springer-Verlag, Vienna, 1963).

(5) E. Dempsey, Phil. Mag. 8, 285 (1963).

(6) A. R. Ubbelohde, Trans. Faraday Soc. 28, 284 (1931).

(7) Ya. S. Umanskii, Ann. sect. anal. phys.-chim., Inst. chim. gén. (USSR) 16, No. 1. 127 (1943).

(8) R. E. Rundle, Acta Cryst. 1, 180 (1948).

(9) R. Kiessling, Acta Chem. Scand. 4, 209 (1950).

(10) R. Kiessling, Met. Rev. 2, 77 (1957).

(11) D. A. Robins, Powder Met. 1/2, 172 (1958).

(12) H. Bilz, Z. Physik 153, 338 (1958).

(13) J. C. Slater and G. F. Koster, Phys. Rev. 94, 1498 (1954).

(14) P. Costa and R. R. Conte in Nuclear Metallurgy Symposium (Metallurgical Society of AIME, New York, 1964), Vol. 10, p. 3.

(15) G. C. Fletcher, Proc. Phys. Soc. (London) A65, 192 (1952).

(16) V. Ern and A. C. Switendick, Phys. Rev. 137, A1927 (1965).

(17) R. G. Lye and E. M. Logothetis, Phys. Rev. 147, 622 (1966).

(18) N. F. Mott and H. Jones, Theory of the Properties of Metals and Alloys (Dover Publications, New York, 1958).

(19) A. H. Wilson, The Theory of Metals (University Press, Cambridge, 1953), 2nd ed.

(20) J. R. Reitz, in Solid State Physics, edited by F. Seitz and D. Turnbull, (Academic Press Inc., New York, 1955) Vol. 1, p. 1 ff.

(21) A. J. Dekker, Solid State Physics (Prentice-Hall, Englewood Cliffs, New Jersey, 1957).

(22) A. Nussbaum, in Solid State Physics, edited by F. Seitz and D. Turnbull, (Academic Press Inc., New York, 1966), Vol. 18, p. 165 ff.

(23) M. Miasek, Phys. Rev. 107, 92 (1957).

(24) W. S. Williams, Phys. Rev. 135, A505 (1964).

(25) J. Piper, Ref. 11, p. 29.

(26) W. S. Williams, Bull. Am. Phys. Soc. 7, 174 (1962).

(27) R. G. Lye, J. Phys. Chem. Solids 26, 407 (1965).

(28) F. J. Morin, Bell System Technical J. 37, 1047 (1958).

(29) G. L. Humphrey, J. Am. Chem. Soc. 73, 2261 (1951).

(30) W. A. Chupka, J. Berkowitz, C. F. Giese, and M. G. Inghram, J. Phys. Chem. 62, 611 (1958).

(31) D. R. Stull and G. C. Sinke, Thermodynamic Properties of the Elements (American Chemical Society, Washington, D. C., 1956).

(32) K. Ruedenberg, Rev. Mod. Phys. 34, 326 (1962).

(33) J. B. Goodenough, Phys. Rev. 120, 67 (1960).